Helmholtz-Zentrum
hereon

Final Draft
of the original manuscript

Wang, J.; Rahman, M.; Abetz, C.; Abetz, V.:
Tuning the size selectivity of isoporous membranes for protein fractionation via two scalable post treatment approaches.
In: Journal of Membrane Science. Vol. 614 (2020) 118535.

First published online by Elsevier: 29.07.2020

https://dx.doi.org/10.1016/j.memsci.2020.118535

Tuning the size selectivity of isoporous membranes for protein fractionation via two scalable post treatment approaches

Jiali Wang[1], Md. Mushfequr Rahman[1], Clarissa Abetz[1], Volker Abetz[1,2]*

[1]Helmholtz-Zentrum Geesthacht, Institute of Polymer Research, Max-Planck-Str. 1, 21502 Geesthacht, Germany

[2]Universität Hamburg, Institute of Physical Chemistry, Martin-Luther-King-Platz 6, 20146 Hamburg, Germany

*Corresponding author. Email address: volker.abetz@hzg.de

Abstract

The molecular design of block copolymer membranes has been widely used as a toolbox to explore the functionality and pore size of the membranes. However, the study of membrane performance as a function of systematic change of the pore size has not been widely explored so far. We prepared an integral asymmetric isoporous membrane on the example of polystyrene-*block*-poly(2-hydroxyethyl methacrylate) (PS-*b*-PHEMA) membranes using an easily scalable method which combines the block copolymer self-assembly and nonsolvent induced phase separation. The pore size of the PS-*b*-PHEMA membrane was tuned via two post treatment methods, a chemical postmodification by urethane chemistry and a physical post treatment by thermal annealing, respectively. At pH 7.4 bovine serum albumin (BSA), hemoglobin (Hb) and catalase (Cat) do not adsorb on the prepared membranes. The retention of BSA, Hb and Cat from their aqueous solution was investigated and the ideal selectivities of three protein pairs $\psi_{BSA/Hb}$, $\psi_{BSA/Cat}$ and $\psi_{Hb/Cat}$ were calculated. The $\psi_{BSA/Cat}$ and $\psi_{Hb/Cat}$ of the postmodified membranes were significantly higher than those of the PS-*b*-PHEMA membrane. This study is the first to demonstrate that the size selectivity of a SNIPS membrane can be enhanced by controlled physical and chemical post treatment of a SNIPS membrane.

1. Introduction

The quest of porous membranes having the desired morphology and functionality for fractionation of proteins remains a vibrant research topic in spite of the extensive development of membrane technology in this regard over several decades.[1-7] Compared to other protein separation techniques (e.g. chromatography, adsorption), the benefits of membrane separation due to high throughput, mild operating conditions and ease of scalability are well accepted.[2, 8] Separation of proteins by ultrafiltration membranes is a complex process which is influenced by many factors, such as pore size distribution and porosity of the membrane, electrostatic interaction between the membrane and the proteins, protein-protein interactions, pH and ionic strength of the protein solution, trans-membrane pressure, shear rate at the membrane surface, concentration polarization, etc.[8, 9] The size selectivity is a crucial factor in the success of membrane protein separation. The broad pore size distribution of the conventional membranes fabricated by non-solvent-induced phase separation (NIPS) is a bottleneck to achieve the sufficient size selectivity for protein fractionation.[10] Therefore, researchers have extensively explored the electrostatic interactions to enhance the selectivity by optimizing the type of charge (i.e. positive or negative) and charge density of the membrane together with the pH and ionic strength of the protein solution.[11-17] Meanwhile several strategies have been reported to fabricate isoporous membranes (i.e. membranes with narrow pore size distribution) by taking advantage of block copolymer (BCP) self-assembly.[6, 18, 19] Although the isoporous membranes are expected to have better size selectivity or sharper molecular weight cut-off compared to conventional non-isoporous membranes, due to lack of empirical demonstration it has not been convincingly established so far. In 2017 Zhou *et al.* have correctly stated - "*Previous studies have demonstrated the ability to fabricate nanoporous membranes with well ordered pores, narrow pore size distribution, and high pore density using self-assembled BCPs. However, tuning the pore size to create size selectivity by design is still a major challenge in the field.*"[6]

The combination of BCP self-assembly with conventional nonsolvent induced phase separation (SNIPS) is well-known as a one-step, easily scalable membrane fabrication method.[18, 20] The integral asymmetric isoporous membranes prepared by SNIPS have earned a reputation as potential next generation membranes for protein separation.[21-25] Since the first SNIPS membrane was fabricated using polystyrene-*block*-poly(4-vinylpyridine) (PS-*b*-P4VP) in 2007[18], tremendous efforts have been made to further develop the fabrication techniques in order to prepare SNIPS membranes both in flat sheet[26, 27] and hollow fiber[28-31] geometry. The molecular design of BCPs for fabrication of membranes having diverse chemical functionality and pore sizes have been extensively explored. The feasibility of the formation of integral asymmetric isoporous membranes by SNIPS method have been demonstrated using diverse block copolymers, such as poly(*tert*-butylstyrene)-*block*-poly(4-vinylpyridine)[32], poly(4-trimethylsilylstyrene)-*block*-poly(4-vinylpyridine)[32], polystyrene-*block*-poly(2-vinylpyridine)[33], polystyrene-*block*-poly(ethylene oxide)[34], polystyrene-*block*-poly(2-vinylpyridine)-*block*-poly(ethylene oxide)[35], polyisoprene-*block*-polystyrene-*block*-poly(4-vinylpyridine)[36], polyisoprene-*block*-polystyrene-*block*-poly(*N,N*-dimethylacrylamide)[37], polystyrene-*block*-poly(4-(2-hydroxyethyl-thio)-2-methyl butene-*random*-4-(2-hydroxyethyl-thio)-3-methyl butene-*random*-isoprene)[38], poly(4-(2-hydroxyethyl-thio)-2-methyl butene-*random*-4-(2-hydroxyethyl-thio)-3-methyl butene-*random*-isoprene)-*block*-polystyrene-*block*-poly(4-vinylpyridine)[39], polystyrene-*block*-poly(2-hydroxyethyl methacrylate) (PS-*b*-PHEMA)[40], polystyrene-*block*-poly(2-hydroxyethyl methacrylate-*random*-2-(succinyloxy)ethyl methacrylate)[25], polystyrene-*block*-poly(glyceryl methacrylate)[41] and polystyrene-*block*-poly(4-vinylpyridine)-*block*-poly(solketal methacrylate) (PS-*b*-P4VP-*b*-PSMA)[42], etc. The rich polymer library of the SNIPS membranes provides an option to explore chemical functionality along the pore wall of the isoporous layer. Moreover, various reaction routes have been successfully implemented for selective

postmodification of the pore-forming blocks of the SNIPS membranes. Several facile ways were introduced to tune the pore size of the SNIPS membranes. For example- changing the molecular weight and the composition of BCPs[43], blending BCPs of different molecular weights and compositions[44], selective chemical postmodification of pore-forming block[45], thermal annealing[45], incorporating small molecules in casting solution[23], deposition of gold or aluminum oxide[20, 46], etc.

In spite of the development of rich polymer library, membrane postmodification techniques and facile strategies to tune the pore size of the isoporous layer of the SNIPS membrane, there remains a lack of understanding of the retention behavior of the membranes having different pore functionality and pore sizes. So far the retention of a series of membranes having different dry state pore size has been investigated only for PS-*b*-P4VP membranes[22, 47] while the retention of a series of membrane having different effective pore size in hydrated state is only reported for quaternized PS-*b*-P4VP membranes.[48] Clodt *et al*.[47] studied the water flux and poly(ethylene glycol) (PEG) retention of a series of PS-*b*-P4VP membranes having pore diameter in the range 17-86 nm. The water flux of this series of membranes increased with the surface pore size of the membrane while the PEG retention was independent of pore size. It indicated a strong contribution of the spongy substructure of the membranes on PEG retention. Hahn *et al*.[22] investigated the adsorption, permeability and diffusivity of lysosome, myoglobin, hemoglobin (Hb), catalase (Cat) and ferritin through a series of PS-*b*-P4VP membranes having pore diameter between 17-53 nm. Although the PS-*b*-P4VP membranes showed promising selectivities of several protein pairs, the role of pore size in the separation was not clear due to strong adsorption of the proteins at the surface of the membrane. To be able to understand the influence of pore size it is important to study the retention of the model proteins which do not have a tendency to adsorb at the surface of the membrane at the operating pH. The most widely studied model protein bovine serum albumin (BSA) tends to adsorb on the surface of PS-*b*-P4VP membranes.[49] Tripathy *et al*.[50] found if the P4VP block of the PS-*b*-P4VP is quaternized with alkyl halide the adsorption of BSA at the surface of the membrane increases both at pH 7 and pH 4. Shevate *et al.*[51] selectively etched out the P4VP block of PS-*b*-P4VP SNIPS membrane by quaternization of the P4VP blocks with methyl iodide followed by degradation of the quaternized P4VP block in an alcoholic alkaline medium. The permeation of BSA through the membranes gradually increased with the time of alcoholic alkaline treatment which resulted in high size based selectivities of BSA over globulin-γ. Saleem *et* al.[42] found the BSA retention of a PS-*b*-P4VP-*b*-PSMA membrane having a dry state pore diameter of 26 nm before and after hydrolysis is 90% and 20%, respectively. Due to hydrolysis the poly(solketal methacrylate) block converts into a hydroxyl group containing poly(glyceryl methacrylate) block which prevents the fouling of the membrane by BSA and consequently the retention drops significantly. In this work we have investigated the adsorption and retention of three bovine proteins BSA, Hb and Cat by two series of SNIPS membranes having a hydroxyl group containing pore-forming block and dry state pore size between 9 nm to 34 nm. The membranes were prepared on a nonwoven support using PS-*b*-PHEMA block copolymer and they were subsequently postmodified either by conversion with an isocyanate to form urethane containing side groups or by thermal annealing.[45] To benchmark the potential of the prepared membranes for protein fractionation the ideal selectivity of the three protein pairs (BSA/Hb, BSA/Cat and Hb/Cat) for the prepared membranes are compared with 22 commercial and in-house prepared isoporous and non-isoporous membranes.

2. Experimental

2.1. Reagents and materials

Tetrahydrofuran (THF), N,N-dimethylformamide (DMF), 1,4-dioxane (DOX), *n*-hexane, hydrochloric acid fuming 37% (HCl) and methanol were ordered from Th. Geyer (Renningen, Germany) and Merck

Millipore (Darmstadt, Germany). Styrene, 2-(trimethylsilyloxy)ethyl methacrylate (HEMA-TMS), lithium chloride (LiCl), *sec*-butyl lithium (*sec*-BuLi) (1.4 M in cyclohexane), di-n-butylmagnesium ($MgBu_2$) (1.0 M in heptane), 1,1-diphenylethylene (DPE), triethylaluminium (TEA) (1.0 M in hexane), calcium hydride (CaH_2), basic aluminum oxide, benzoic anhydride, magnesium acetate ($MgAc_2$), coper acetate ($CuAc_2$), ethyl isocyanate, perfluoro(methyl cyclohexane) and proteins were purchased from Sigma-Aldrich (Schnelldorf, Germany). Deuterated solvents were purchased from Deutero GmbH (Kastellaun, Germany). All chemicals and solvents were reagent grade. TH100 (Hirose Paper Mfg Co., Ltd, Japan) is 100% polyester-fiber wet-laid nonwoven support. AWA (AWA Paper & Technological Company, Inc., Japan) is wet-type nonwoven fabric made from 100% polyester fiber. FO nonwoven support (Hirose Paper Mfg Co., Ltd, Japan) is composed of polyethylene and polypropylene. AS030 nonwoven support (Asahi Kasei Co., Japan) is made from polyester consisting of 3 layers (Supanbond, Meltblow and Supanbond). (Details in Supporting Information, Fig. S5)

2.2. Polymer synthesis

PS-*b*-PHEMA diblock copolymer was successfully synthesized by sequential anionic polymerization following a subsequent hydrolysis of the trimethylsilyloxy group following a protocol reported before[45, 52] (detail description in Supporting Information).

2.3. Membrane fabrication

The polymer solution of PS-*b*-PHEMA copolymers was prepared in a THF/DMF/DOX ternary solvent mixture with or without the addition of salts. After stirring for 48 h the polymer solution was manually casted using a doctor blade with different gap heights in the range of 50~200 μm on a glass plate or a polyester nonwoven support. After casting the prepared membranes were immersed in a water bath for 20 min to make sure the complete exchange between the solvent mixture and water. Since PHEMA segments are very sensitive to the humidity, the relative humidity of air (RH) was precisely controlled below 20% by using the glove box with N_2 flowing during the whole process of casting.[45] The membranes were dried 4 days under vacuum at 50 °C to remove all residual solvents.

2.4. Postmodification by urethane chemistry

The PS-*b*-PHEMA membrane reacted with equivalent ethyl isocyanate in excessive PFMCH at 65 °C for a series of reaction time under argon.[45] The membranes were subsequently washed with ethanol and water to drain off any unreacted molecule and dried in a vacuum oven at 50 °C for 4 days.

2.5. Post treatment by thermal annealing

The PS-*b*-PHEMA membrane was immersed in excessive PFMCH at 75 °C for a series of annealing time and subsequently quenched in water at room temperature and dried in a vacuum oven at 50 °C for 4 days.[45]

2.6. Determination of molecular weight and composition of block copolymers

To facilitate the characterization of PS-*b*-PHEMA block copolymers, the hydroxyl groups of the PHEMA segments were protected by benzoic anhydride.[45] Dispersity index (Đ) and molecular weights of the PS-*pre* and the benzoylated PS-*b*-PHEMA (PS-*b*-P(HEMA-Bz)) diblock copolymers were determined by size exclusion chromatography (SEC). The measurements were performed at 25 °C in THF using 5 μm PSS SDV gel columns at a flow rate of 1.0 mL min^{-1} (VWR-Hitachi 1110 pump,

Hitachi, Darmstadt, Germany). A Chromaster 5410 refractive-index detector (λ=254 nm) was used with a PS calibration. The characteristic peaks of polymers were quantitatively determined by proton nuclear magnetic resonance (^{1}H-NMR) (300 MHz, Bruker, Rheinstetten, Germany) using DMF-d7.

2.7. Morphological investigation

The bulk morphology of block copolymer was studied by transmission electron microscopy (TEM) (Tecnai G^2 F20, FEI, Eindhoven, The Netherlands) operated at 120 kV in bright-field mode. (Supporting Information) The membrane morphology was investigated by scanning electron microscopy (SEM) (LEO Gemini 1550 VP from Carl ZEISS, Oberkochen, Germany) at an acceleration voltage of 3 kV. To preserve their microscopic morphology, cross-sections of the membranes were prepared by freezing the samples in liquid nitrogen and cracking. The samples were coated with 1.0 or 1.5 nm thick platinum. The average pore diameter (D), the center-to-center distance of two neighboring pores (d), the height of cylinder (h) and the surface porosity (the ratio of pore area per unit area of one SEM image) were measured by ImageJ 1.46 (Wayne Rasband, National Institute of Health, Madison, WI, USA) and analySIS (Olympus Soft Imaging Solutions GmbH, Münster, Germany) on the basis of the SEM results.

2.8. Viscosity of polymer solutions

The dynamic viscosity of polymer solution was measured with the rotational viscometer EuroPhysics Rhoe2000 (RheoTec, Dresden, Germany) using a C25-1 cone/plate geometry. The measurements were performed at a constant shear rate of 200 s^{-1} at 20 °C.

2.9. Streaming zeta potential at the surface of the membranes

Zeta potential measurements were measured by the SurPASS Electro-kinetic Analyzer (Anton-Paar KG, Graz, Austria). For each sample, four streaming potentials were measured at each pH value. The mean value of these data was used to calculate the zeta-potential/pH function.

2.10. Surface water contact angle

Water contact angle at the surface of the membranes were measured with 1 µL deionized water droplets using a KRUESS Drop Shape Analysis System DSA 100 (FEI part of Thermo Fisher Scientific, Kawasaki, Japan). Each sample was measured at least three times at room temperature.

2.11. Water permeance

The pure water permeance measurements were conducted in a dead-end mode at a constant feed pressure of 2 bar at 20 °C for 3 hours using the test unit as shown in Fig. S12 (Supporting Information). These studies were performed by using demineralized water which had an electrical conductivity of ≈ 0.055 µS cm^{-1}. The volume change of pure water permeance (ΔV) was measured gravimetrically over a balance every 60 sec and pressure was measured as well. The effective membrane area (A) was 1.77 cm^2. All the membranes were soaked in demineralized water for 24 h before measurement to ensure the sufficient swelling of membrane. All experiments were performed at least three times by using three individual samples. The water permeance (J) is calculated as:

$$J = \frac{\Delta V}{A \cdot \Delta t \cdot \Delta p} \quad (1)$$

Where, ΔV is the volume change of water permeance between two mass measurements, A is the effective membrane area, Δt is the time interval between two mass measurements, Δp is the trans-membrane pressure.

2.12. Protein adsorption

Adsorption experiments were conducted with BSA, Hb and Cat. 1 g L^{-1} single protein solution was prepared in a phosphate-buffered saline (PBS, pH = 7.4). The sample of membrane in the diameter of 2 cm was immersed in 2 mL protein solution in a sealed vial. The vials were placed on the shaking bed at 90 rpm for 24 h at 25 °C to ensure the membrane reached the equilibrium of adsorption. After that, the samples were rinsed twice with 2 mL of the PBS buffer solution for 10 minutes at 90 rpm at 25 °C. The mass of proteins in each solution was calculated based on the concentrations of the protein which were determined by GENESYS 10S UV-vis spectrophotometer (Thermo Scientific, Waltham, USA). The protein adsorption on the membrane was calculated as follows:

$$protein\ adsorption = \frac{m_0 - (m_1 + m_{w1} + m_{w2})}{A} \quad (2)$$

where m_0 is the protein mass before the adsorption experiment, m_1 is the protein mass after the adsorption experiment, and m_{w1} and m_{w2} are the protein masses in the rinsing buffer. The adsorption value is normalized by the membrane area (A).

2.13. Protein retention

The protein retention measurements were accessed in a dead-end mode with continuously stirring under a trans-membrane pressure of 2 bar at 20 °C using the test unit as shown in Fig. S13 (Supporting Information). The membrane filtration cell (Supporting Information, Fig. S13b) is purchased from EMD Millipore™ and refitted to our house-made devices. The effective membrane area was 1.77 cm^2. Each measurement was conducted in triplicate at least. The retention properties of the membranes were investigated using BSA, Hb and Cat. The feed solution of proteins was all freshly prepared in a PBS buffer solution at pH = 7.4 for retention measurement. The PBS solution was first supplied to the membranes for 1 h at the trans-membrane pressure of 2 bar in order to exclude the influence of buffer, and then the 1 g L^{-1} feed solution of proteins was provided at the same pressure for 2 h. The concentration of proteins in the feed (C_f) and permeate (C_p) was determined by GENESYS 10S UV-vis spectrophotometer (Thermo Scientific, Waltham, USA) and the retention ratio of proteins was calculated following the equation shown below:

$$R\% = \left(1 - \frac{C_p}{C_f}\right) \times 100\% \quad (3)$$

Where, C_p and C_f are concentrations of proteins in permeate and feed, respectively.

Solute transmission is usually expressed in terms of the observed percentage transmission (τ_{Obs}).[53]

$$\tau_{Obs} = \frac{C_p}{C_f} \times 100 \quad (4)$$

The ideal selectivity (ψ) of one protein from another one is expressed as:[53]

$$\psi = \frac{(\tau_{Obs})_i}{(\tau_{Obs})_j} \quad (5)$$

where $(\tau_{Obs})_i$and $(\tau_{Obs})_j$are the observed percentage transmission of two different proteins.

3. Results and Discussion

3.1. PS-*b*-PHEMA membrane fabrication via SNIPS

Empirical optimization of the casting parameters is an integral part of fabrication of an asymmetric membrane having hexagonally close-packed vertically aligned isoporous channels on top of a highly porous spongy sublayer by SNIPS method.(Fig. 1a) The casting parameters include the concentration of casting solution, the composition of the solvent system, the evaporation time prior to the precipitation bath and the addition of additives, temperature, humidity, etc. In a previous study we reported the casting parameters of a free-standing integral asymmetric isoporous membrane using a PS_{91}-*b*-$PHEMA_9^{97k}$ where the subscripts denote the weight fractions in % and the superscripts the corresponding molecular weight of the block copolymer in kg mol^{-1}.[45] In order to ensure the mechanical robustness of the membrane during the filtration process it is important to cast the integral asymmetric membranes on top of a macroporous nonwoven support. However, it was not possible to obtain the desired PS_{91}-*b*-$PHEMA_9^{97k}$ SNIPS membrane on a nonwoven support. Due to low viscosity the casting solution penetrated through the TH100, AWA and FO nonwoven supports while the PS_{91}-*b*-$PHEMA_9^{97k}$ layer delaminated from the AS030 nonwoven support (Supporting Information, Fig. S5). Therefore, in this work we successfully prepared the higher molecular weight PS_{87}-*b*-$PHEMA_{13}^{180k}$ (Supporting Information, Fig. S1-S4) and used it for membrane casting in order to solve such problems. At first, we optimized the casting parameters for a PS_{87}-*b*-$PHEMA_{13}^{180k}$ free-standing membrane. Fig. 1b-d shows the influence of the composition of the ternary solvent mixture of DMF/THF/DOX on the surface morphology prepared from 18 wt % PS_{87}-*b*-$PHEMA_{13}^{180k}$ solutions. Randomly distributed open porous structures are visible on the surface of the membranes cast from DMF/THF/DOX (1:2:1) and DMF/THF/DOX (1:1:2) using an evaporation time of 10 s prior to transfer into the precipitation bath. The membranes cast from DMF/THF/DOX (1:1:1) using the same evaporation time have a more open porous surface morphology compared to those cast from the other two ternary solvent mixtures. According to the solubility parameters (Table 1), THF and DOX are more selective for the PS block while DMF is more favorable for the PHEMA block. As THF is more volatile than DOX and DMF, the self-assembly of block copolymer is highly driven by the evaporation of THF and meanwhile DMF keeps the PHEMA block in a relatively swollen state. DMF/THF/DOX (1:1:1) has the highest DMF content among the three ternary solvent mixtures. The increase of DMF content in the ternary solvent mixture has effectively enhanced the microphase separation of the blocks by selectively swelling the PHEMA block, leading to a highly open porous morphology. Free-standing membranes were cast on a glass plate from PS_{87}-*b*-$PHEMA_{13}^{180k}$ solutions in DMF/THF/DOX (1:1:1) by changing the concentration of the casting solution and the evaporation time prior to the precipitation bath (Supporting Information, Fig. S6). The desired integral asymmetric isoporous structure was not obtained. We introduced $MgAc_2$ and $CuAc_2$ as additives to the casting solution as the addition of salts can facilitate the formation of an isoporous top layer of the SNIPS membranes (Supporting Information, Fig. S6).[40, 54] $CuAc_2$ significantly improved the self-assembly of the polymer chains leading to hexagonal packed open pores. Copper should have a stronger ability to form interactions with PHEMA than magnesium which might have facilitated the membrane formation using the casting solutions containing $CuAc_2$ additive. By optimizing the concentration of polymer solution and $CuAc_2$, the free-standing integral asymmetric isoporous membrane was successfully prepared from a 20 wt % PS_{87}-*b*-$PHEMA_{13}^{180k}$ polymer solution containing 0.3 wt % $CuAc_2$ in DMF/THF/DOX (1:1:1) at the evaporation time of 15

s. Fig. 1e and f shows a scanning electron micrograph of the membrane surface and a photograph of the successfully prepared free-standing PS_{87}-*b*-$PHEMA_{13}^{180k}$ SNIPS membrane, respectively.

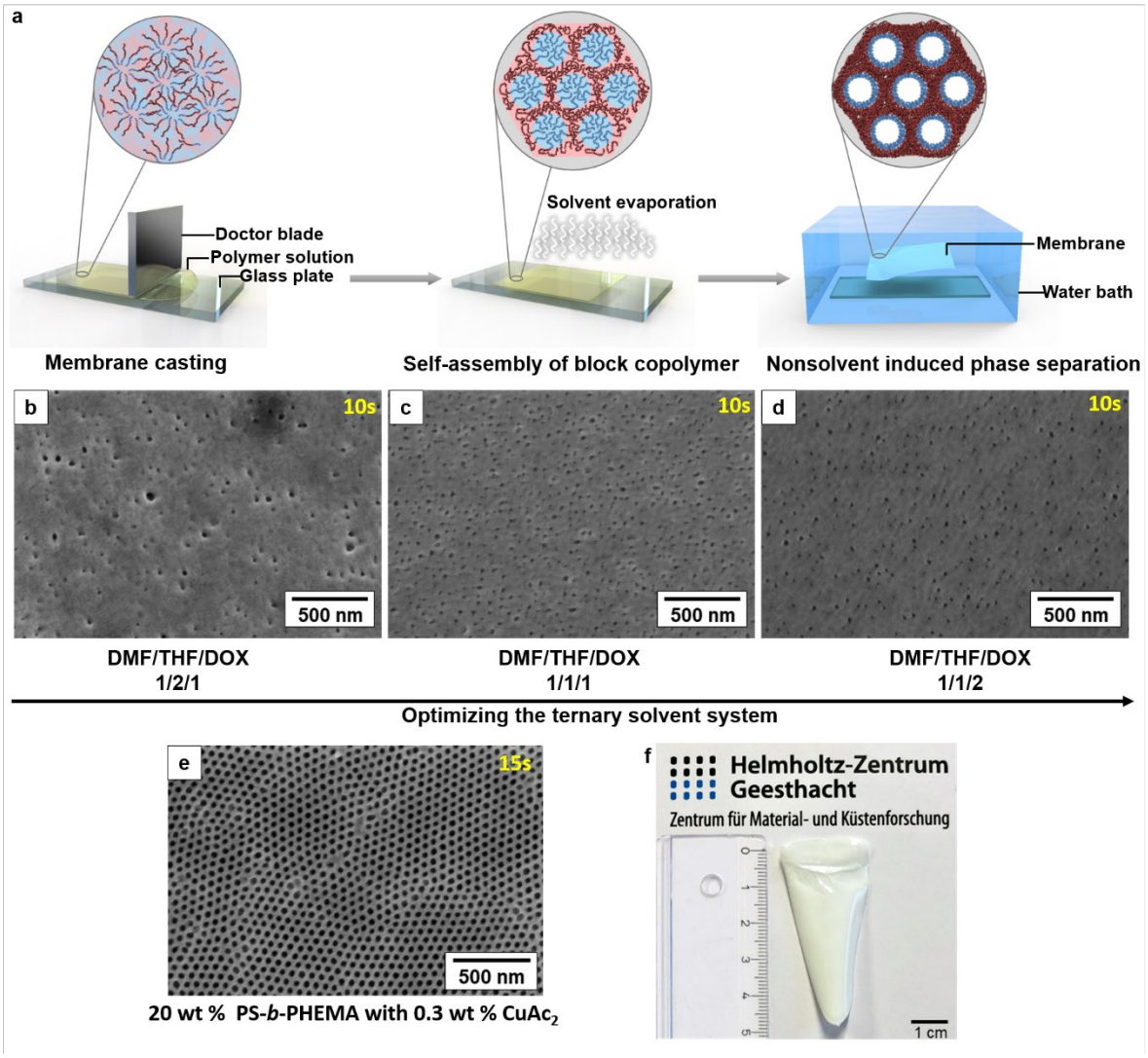

Fig. 1. a) Schematic of the SNIPS process. SEM images of membrane surface prepared from 18 wt % PS_{87}-*b*-$PHEMA_{13}^{180k}$ polymer solutions - b) in DMF/THF/DOX (1:2:1) at the evaporation time of 10 s; c) in DMF/THF/DOX (1:1:1) at the evaporation time of 10 s; d) in DMF/THF/DOX (1:1:2) at the evaporation time of 10 s. e) SEM image of membrane surface prepared from 20 wt % polymer solution containing 0.3 wt % $CuAc_2$ in DMF/THF/DOX (1:1:1) at the evaporation time of 15 s cast on a glass plate. f) Photograph of the free-standing PS_{87}-*b*-$PHEMA_{13}^{180k}$ membrane.

Table 1
Hansen Solubility parameters of solvents and homopolymers.[55-57]

Polymers	Solubility parameter [$MPa^{0.5}$]	Solvents	Solubility parameter [$MPa^{0.5}$]
PS	20.1	THF	19.5

PHEMA	23.3	DMF	24.9
		DOX	20.5

The next step was to cast an integral asymmetric isoporous PS_{87}-*b*-$PHEMA_{13}^{180k}$ membrane on top of a nonwoven support in order to ensure the mechanical integrity of the membrane during water permeance and protein retention measurements. However, the isoporous surface structure was completely lost when the membrane was cast on the TH100 nonwoven support (Fig. 2a-b). In order to solve this unexpected problem, we have further investigated the influence of concentration of the polymer solution and the $CuAc_2$ content when the membrane was cast on a nonwoven support. Some of these membranes had inhomogeneous isoporous surface morphology where only some parts of the membrane surface had the desired hexagonally packed isoporous structure (Supporting Information, Fig. S7). A change of the gap height of the doctor blade between 50-200 µm did not solve the problem of surface inhomogeneity (Supporting Information, Fig. S8). In fact, the membranes obtained from small gap heights e.g. 50 µm had a completely nonporous surface morphology. As we could not prevent formation of an inhomogeneous surface morphology using the casting solutions containing $CuAc_2$ additives, we had to find an optimum condition to prepare the desired PS_{87}-*b*-$PHEMA_{13}^{180k}$ membrane on the nonwoven support using a casting solution without additives. The desired membrane was finally obtained from a 24 wt % PS_{87}-*b*-$PHEMA_{13}^{180k}$ solution in DMF/THF/DOX (1:1:1) at the evaporation time of 20 s (Fig. 2d). The viscosity of this casting solution was more than double compared to that used to obtain the free-standing PS_{87}-*b*-$PHEMA_{13}^{180k}$ membrane (Fig. 2c). Using these casting parameters several membranes having areas greater than 100 cm^2 were fabricated (Fig. 2e). Each of these membranes had the integral asymmetric isoporous morphology all over the area. The membranes were also mechanically sufficiently robust to study the water flux and protein retention properties which are discussed in the following sections together with the post treated membranes.

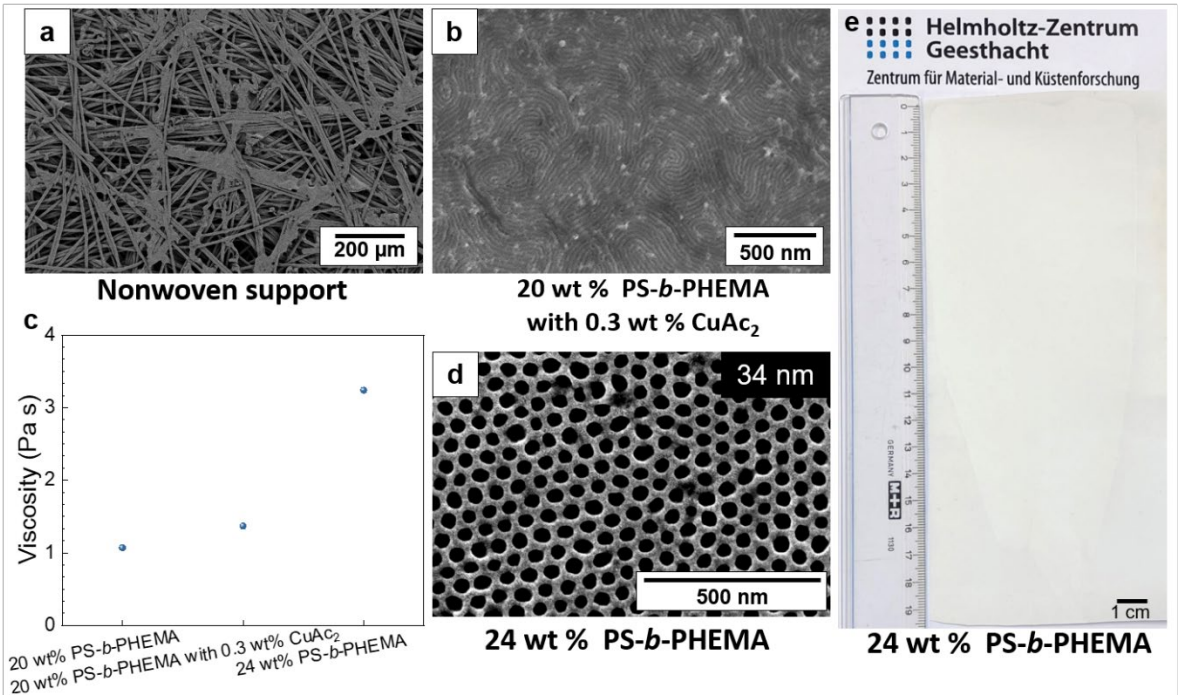

Fig. 2. SEM images of a) the surface of nonwoven support; b) PS_{87}-*b*-$PHEMA_{13}^{180k}$ membrane cast on a nonwoven support from 20 wt % polymer solution containing 0.3 wt % $CuAc_2$ in DMF/THF/DOX

(1:1:1) at the evaporation time of 15 s. c) Viscosity of the casting solutions. d) SEM image of membrane surface prepared from 24 wt % PS_{87}-*b*-$PHEMA_{13}^{180k}$ polymer solution in DMF/THF/DOX (1:1:1) at the evaporation time of 20 s cast on a nonwoven support. e) Photograph of PS_{87}-*b*-$PHEMA_{13}^{180k}$ membrane on nonwoven support.

3.2. Postmodification of PS-*b*-PHEMA membranes by urethane chemistry

Postmodification of PS_{87}-*b*-$PHEMA_{13}^{180k}$ membranes (SH) by urethane chemistry was used to selectively modify HEMA moiety to tune the pore size. It was carried out using ethyl isocyanate in perfluoro(methyl cyclohexane) (PFMCH) at 65 °C to generate polystyrene-*block*-poly(2-hydroxyethyl methacrylate-*random*-2-ethylcarbamoyloxy ethyl methacrylate) (PS-*b*-P(HEMA-*r*-ECEMA)) membranes (Fig. 3).[45] The dry state pore size systematically decreased as a function of reaction time without any significant change of the height of cylindrical pores. It is worth mentioning that the scale of the reaction flask had a significant influence on the reaction time required to achieve a desired pore size (Supporting Information, Fig. S9). The average dry state surface pore diameters and the surface porosities of the PS-*b*-P(HEMA-*r*-ECEMA) membranes after 24 h, 36 h and 48 h reaction (SHE-24h, SHE-36h and SHE-48h) in a 500 ml reaction flask are listed in Table 2. After postmodification of ethyl isocyanate for 48 hours, the average pore diameter of membranes was reduced from 34 ± 0.9 nm down to 9 ± 0.2 nm and the surface porosity accordingly decreased from 24 ± 1.3 % to 5 ± 0.2 % (Fig. 4a-d). The volume of each hexagonal unit of the block copolymer of the isoporous layer as a function of reaction time fits a second-order polynomial relationship (Supporting Information, Fig. S11) which demonstrates the success of controlled dry state pore size reduction via urethane chemistry in a 500 ml reaction flask.

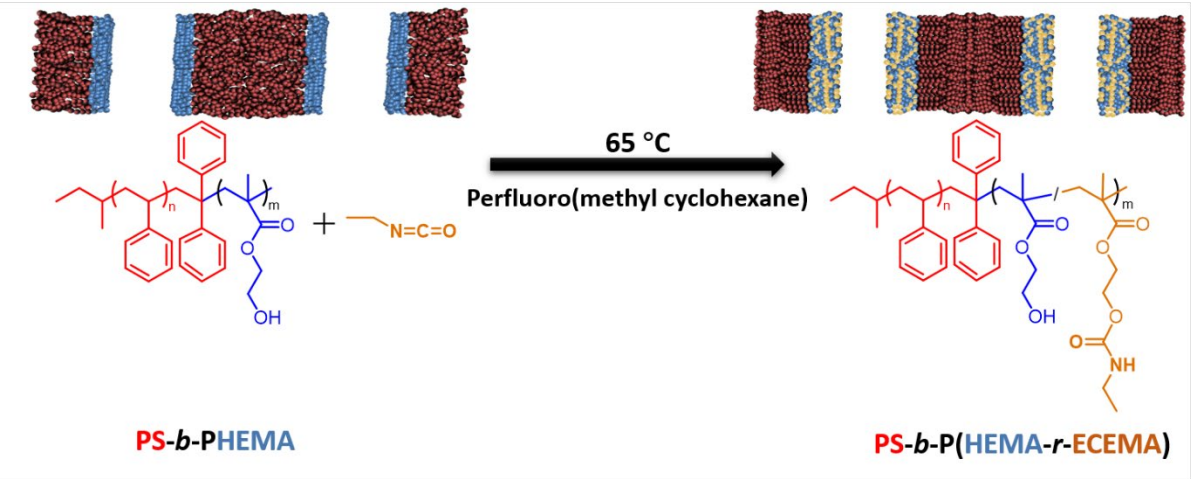

Fig. 3. Synthesis scheme of polystyrene-*block*-poly(2-hydroxyethyl methacrylate-*random*-2-ethylcarbamoyloxy ethyl methacrylate) (PS-*b*-P(HEMA-*r*-ECEMA)) membrane by postmodification of PS-*b*-PHEMA membranes using ethyl isocyanate in perfluoro(methyl cyclohexane) and the schematic presentation of the isoporous top layer of membrane.

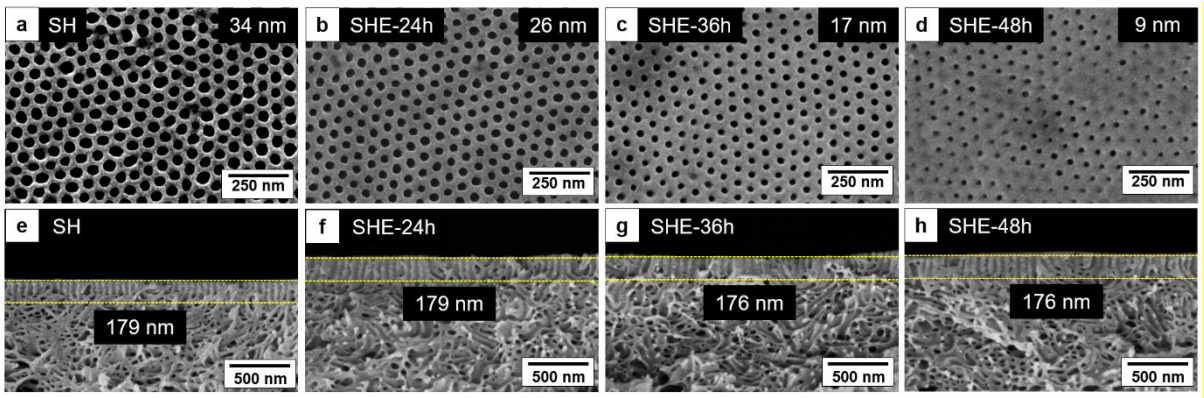

Fig. 4. SEM images of a-d) the surface and e-h) the cross-section of PS-*b*-PHEMA pristine membrane (SH), PS-*b*-P(HEMA-*r*-ECEMA) membranes postmodified by ethyl isocyanate using 500 mL reactor at 65 °C for 24 h (SHE-24h), 36 h (SHE-36h) and 48 h (SHE-48h), respectively.

Table 2

The average pore diameter and surface porosity of PS-*b*-PHEMA pristine membrane and PS-*b*-P(HEMA-*r*-ECEMA) membranes postmodified by ethyl isocyanate for a series of reaction times.

Acronym of membranes	Polymers	Reaction time [h]	The average pore diameter in a dry state [nm]	Surface porosity in a dry state [%]
SH	PS-*b*-PHEMA	0	34 ± 0.9	24 ± 1.3
SHE-24h	PS-*b*-P(HEMA-*r*-ECEMA)	24 h	26 ± 0.5	15 ± 0.1
SHE-36h	PS-*b*-P(HEMA- *r*-ECEMA)	36 h	17 ± 0.9	9 ± 0
SHE-48h	PS-*b*-P(HEMA- *r*-ECEMA)	48 h	9 ± 0.2	5 ± 0.2

The surface hydrophilicity of the membranes was investigated by the water contact angle on the membrane surface (Fig. 5b).[58] SH membrane has a low water contact angle due to the hydrophilic –OH group of the PHEMA segments. The introduction of the carbamoyl group in the pore-forming block decreased the hydrophilicity of the membrane which consequently led to the increase of the water contact angle. For an increase of the reaction time between 24 h and 48 h the water contact angle remains unchanged. But the increase of ECEMA content with the reaction time and the subsequent decrease of the dry state pore size had a significant influence on the water permeance through SHE-24h, SHE-36h and SHE-48h, respectively (Fig. 5c). The pore-forming blocks of the prepared membranes swell in a hydrated state. Hence, the effective pore size of the membrane during water flux and protein retention measurements are different from the dry state pore size observed by SEM (schematic representation in Fig. 5a). The extent of swelling of the pore forming block largely depends on the hydrophilic –OH group content. The water permeance of SH is 111 ± 5 L m^{-2} h^{-1} bar^{-1}. (Fig. 5c) SHE-24h has a slightly higher water permeance of 119 ± 4 L m^{-2} h^{-1} bar^{-1}. In SHE-24h the –OH groups are partially substituted by carbamoyl group leading to a less hydrophilic membrane surface as shown in water contact angle. Although the pore size measured by SEM in the dry state is relatively smaller than in SH, the effective

pore size in a swollen state is bigger due to lower swelling of the P(HEMA-*r*-ECMA) blocks compared to the PHEMA blocks resulting in a slightly higher water permeability. With increasing reaction time, the gap between the dry state pore size and the effective pore size becomes smaller due to the increasing ECEMA moieties. The significant drop of water permeance in SHE-36h and SHE-48h is expected to arise from a combined effect of lower hydrophilicity of the pore forming block and lower effective pore size. As the water contact angle at the surface of SHE-24h, SHE-36h and SHE-48h remains unchanged it is likely that the effective pore size of SHE-24h > SHE-36h > SHE-48h. The chemical postmodification has no influence on the streaming zeta potential at the surface of the membranes (Fig. 5d). Similar like SH the postmodified membranes have a strong negative charge in the pH range 6.5-10. The zeta potential gradually approaches zero as the is pH decreased to 3.

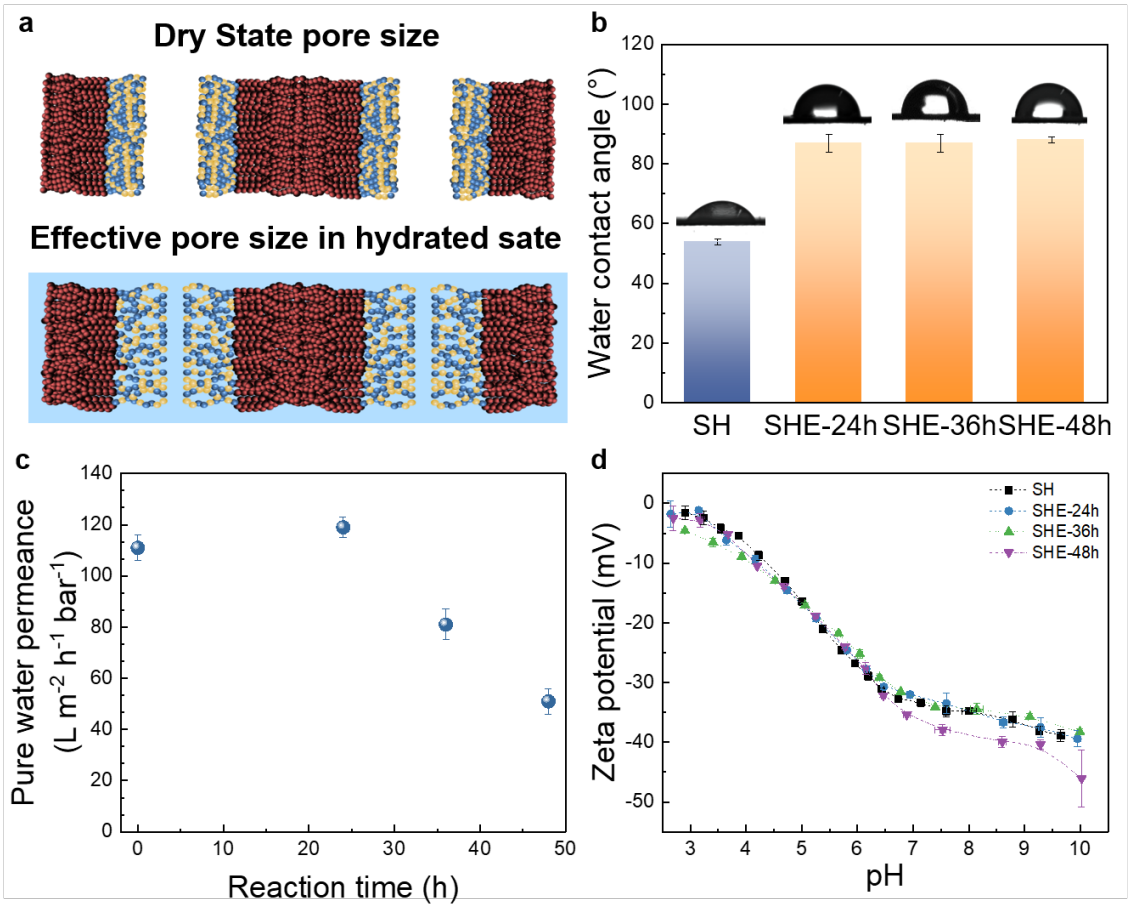

Fig. 5. a) Schematic representation of dry state and hydrated state pores of PS-*b*-P(HEMA-*r*-ECEMA) membranes (SHE-24h, SHE-36h and SHE-48h). Comparison of SH, SHE-24h, SHE-36h and SHE-48h: b) water contact angle at the surface of the membranes, c) water permeance, d) streaming zeta potential at the surface of the membranes.

The physical characteristics of BSA, Hb and Cat are listed in Table S2 (Supporting Information). At pH 7.4, all the proteins are negatively charged since their isoelectric points are below pH 7.4. None of the proteins adsorbed at the membranes upon soaking in the protein aqueous solutions for 24 h as shown in Table S3 (Supporting Information). As the protein retention measurements were done at pH 7.4 for 2h, it is clear that the retention of membranes was not impaired by the static adsorption of proteins. Moreover, as there is no significant difference among the streaming zeta potential (i.e. charge density at the surface of the membrane) it is likely that the difference of protein retentions by SH, SHE-24h,

SHE-36h and SHE-48h are largely dictated by the effective pore size of the membranes in hydrated state. SH retained 45 ± 2 % BSA, 89 ± 2 % Hb and 96 ± 1 % Cat (Fig. 6) from their respective aqueous solutions. Cat with a molecular weight of 250 kDa was highly rejected by the SH membrane due to the size sieving. Since the molecular weights of BSA and Hb are roughly a quarter of Cat, the retention of both proteins is lower than that of Cat. Thus, the effective pore of SH is small enough to reject Cat but bigger than the molecular size of BSA and Hb. Although the molecular weight of BSA and Hb are almost identical SH allows permeation of nearly twice as many BSA compared to Hb. As shown in Table S2, the dimension of BSA (14 nm × 4 nm × 4 nm) is like prolate ellipsoid while that of Hb (7 nm × 5.5 nm × 5.5 nm) is more sphere-like. BSA has the possibility to adopt an orientation so that the long axis of the prolate ellipsoid aligns perpendicular to the surface of the membrane to enter the isoporous cylindrical channels of the membrane. Therefore, the sphere-shaped Hb has less chance to pass through the membrane than BSA. Besides, Hb is less hydrophilic than BSA (Table S2) so BSA is more favorable to pass through the hydrophilic channels of SH. For the postmodified PS-*b*-P(HEMA-*r*-ECEMA) membranes, the retentions of Cat were systematically increased with the increasing of reaction time and there was no permeation of Cat through the sub-10 nm size pores of SHE-48h. For SHE-24h the retention of both BSA and Hb decreased to 34 ± 8 % and 68 ± 10 % respectively. Similar like the implications of trend of water permeance (Fig. 5c) the lower retention of BSA and Hb also suggests SHE-24h has a relatively larger effective pore size compared to SH. SHE-36h and SHE-48h possessed smaller effective pore sizes and resulted in a systematic increase of the retention for both proteins, respectively. Interestingly, among these 4 membranes only for SHE-36h the retention of BSA was significantly higher than that of Hb. It is noteworthy that the permeance of aqueous solution of Hb is higher through SHE-24h but lower through SHE-36h and SHE-48h compared to that through SH. But the permeance of BSA aqueous solution through the membranes gradually decreased with the increasing reaction time. From these observations it is evident that the retention and permeation of BSA and Hb are not only detected by the effective pore size of the membranes. Apart from the different dimensions, the hydrophilic amino acid content of Hb is relatively lower than that of BSA (Supporting Information, Table S2). Moreover, at pH 7.4 BSA has higher negative charges compared to Hb (Supporting Information, Table S2). As all of these features might have contribution to the permeation of the proteins it is difficult to hypothesize the exact reason behind this additional hindrance for BSA permeation through the pores of SHE-24h compared to Hb permeation. The steric hindrance predominates the retention of the membrane as the pore size gradually decreases in SHE-36h and SHE-48h respectively. Finally, no significant difference in the retention and the permeance of the aqueous solutions of BSA and Hb is observed through SHE-48h containing sub-10 nm pores.

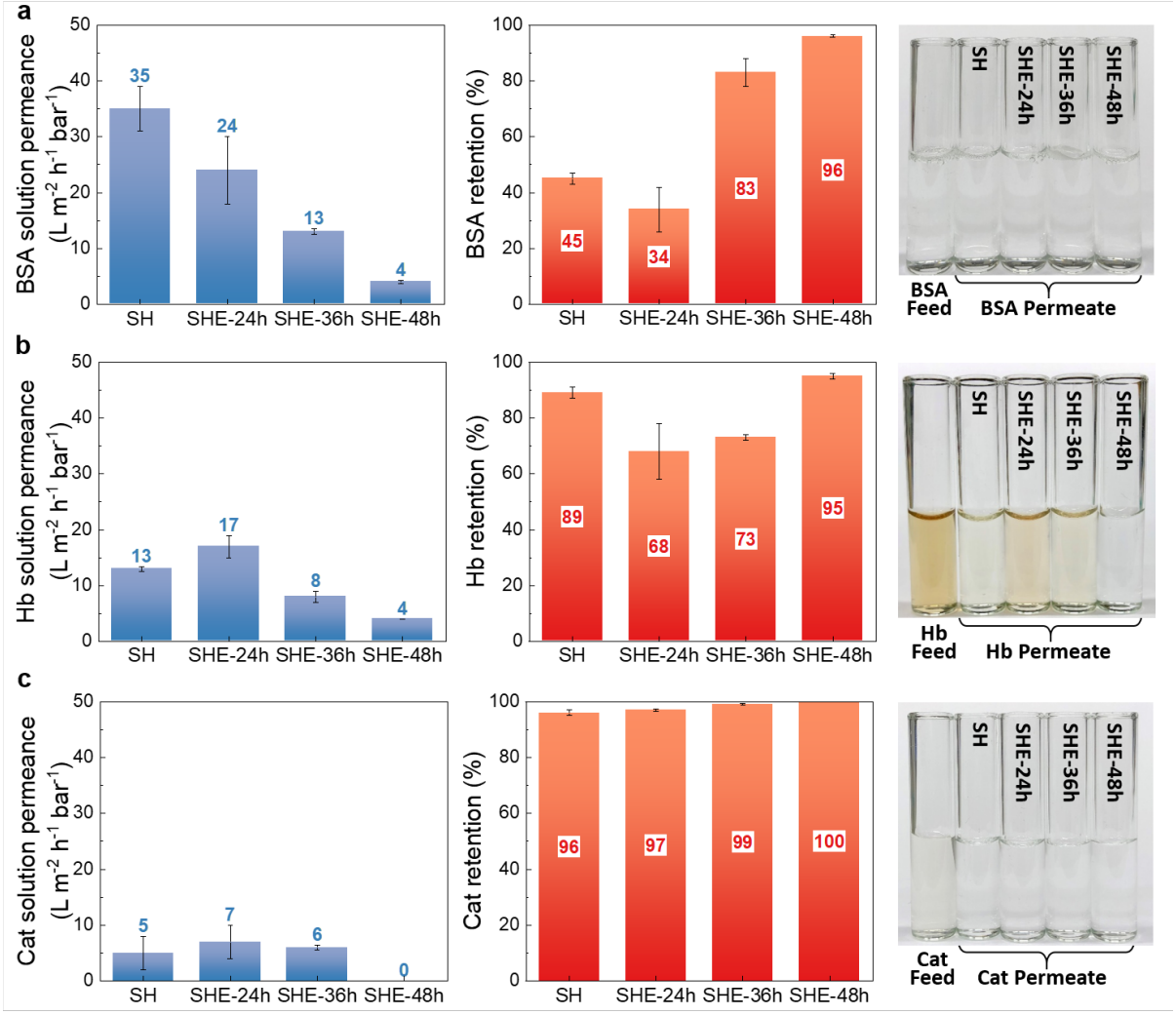

Fig. 6. Protein retention of pristine PS-*b*-PHEMA membrane (SH) and PS-*b*-P(HEMA-*r*-ECEMA) membranes (SHE) for different reaction times.

3.3. Post treatment of PS-*b*-PHEMA membranes by thermal annealing

The pore size of SH was also tuned by thermal annealing following our previously reported method i.e. by immersing the membrane in a PFMCH nonsolvent at 75 °C for different time.[45] In this method the controlled reduction of pore size originates from a controlled relaxation of the polymer segments. As the highly porous top layer is kinetically trapped by SNIPS method and it tends to minimize the surface area to reach an energetically more favorable state. At room temperature such morphological change is not possible as the relaxation time of the polymer segments is infinitely long. At 75 °C the polymer has shorter relaxation time compared to that at room temperature which allows us to tune the pore size of the membrane in this method.[45] In our previous work we reported the systemic reduction of the surface pore size of a free-standing PS_{91}-*b*-$PHEMA_9^{97k}$ membrane by using this method. In this work we also systematically controlled the pore size of SH (i.e. PS_{87}-*b*-$PHEMA_{13}^{180k}$ cast on a nonwoven support) by thermal annealing in a 500 ml flask although the annealing time was longer (Supporting Information, Fig. S10). The SEM micrographs of the surface and cross section of the membranes after 24 h (SH-T24h), 36 h (SH-T36h) and 48 h (SH-T48h) annealing is shown in Fig. 7. The average pore diameter and the height of hollow cylinders in the top layer both decreased

systematically with the increase of annealing time. The dry state surface pore size and surface porosity (obtained from SEM images) of the membranes are listed in Table 3. The volume of each hexagonal unit of the polymer of the isoporous layer as a function of annealing time also fits a second-order polynomial relationship (Supporting Information, Fig. S11).

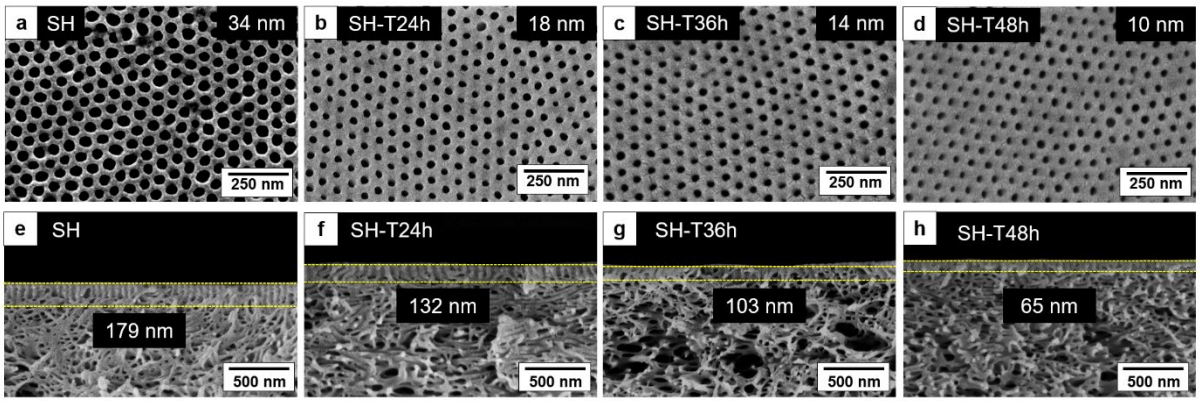

Fig. 7. SEM images of a-d) the surface and e-h) the cross-section of PS-*b*-PHEMA pristine membrane (SH), membranes annealed in perfluoro(methyl cyclohexane) using 500 mL reactor at 75 °C for 24 h (SH-T24h), 36 h (SH-T36h) and 48 h (SH-T48h), respectively.

Table 3
The average pore diameter and surface porosity of PS-*b*-PHEMA pristine membrane and annealed membranes for a series of annealing times.

Acronym of Membranes	Polymers	Annealing time [h]	The average pore diameter in a dry state[nm]	Surface porosity in a dry state [%]
SH	PS-*b*-PHEMA	0	34 ± 0.9	24 ± 1.3
SH-T24h	PS-*b*-PHEMA	24 h	18 ± 0.1	13 ± 0.8
SH-T36h	PS-*b*-PHEMA	36 h	14 ± 0.4	8 ± 0.1
SH-T48h	PS-*b*-PHEMA	48 h	10 ± 0	9 ± 0.7

Fig. 8b shows that the water contact angles at the surface of the thermally annealed membranes (SH-T24h, SH-T36h and SH-T48h) are almost the same as for SH. As the physical treatment has not changed the functionality of membrane, the good surface hydrophilicity of PS-*b*-PHEMA membrane is well preserved. But the pure water permeance through the thermally annealed membranes changed significantly (Fig. 8c). Although there is a systematic decrease of dry state pore size as a function of the annealing time, the water flux through the membrane do not decrease with annealing time. After 24 h annealing, the water permeance increased from 111 ± 5 L m^{-2} h^{-1} bar^{-1} to 271 ± 37 L m^{-2} h^{-1} bar^{-1}. The decrease of the height of cylindrical pores with annealing time may reduce the resistance of water transport through the membrane. But from the trend of water permeation it is clear that the effective pore size of the membranes in a hydrated state SEM (schematic representation in Fig. 8a) does not

follow the similar trend like the dry state pore size determined by SEM. Hence, although the dry state pore size of SH and SH-T24h are 34 ± 0.9 nm and 18 ± 0.1 nm respectively, in a hydrated state the effective pore size of SH-T24h is higher than that of SH. This suggests the PHEMA block of SH has higher freedom to swell compared to that of SH-T24h. As the PS block and PHEMA block are incompatible with each other, the reason for this phenomenon after 24h thermal treatment is not clear. With the increasing of annealing time from 24 h to 48 h, the water permeance of the SH-T36h and SH-T48h systematically decreased. The shorter but smaller water channels of SH-T36h and SH-T48h resulted in the decline of the water permeance. The water permeance of SH-T48h is 123 ± 9 L m^{-2} h^{-1} bar^{-1} which is slightly higher than that of SH (111 ± 5 L m^{-2} h^{-1} bar^{-1}) due to the synergistic influence of the diameter and the length of the soft water channels. Fig. 8d shows the zeta potential of the thermally annealed membranes follows the same trend as SH with the change of pH. A careful inspection shows between pH 6.5 to pH 9 SH-T24h and SH-T48h have slightly more negative zeta potential compared to SH and SH-36h. As there is no regular trend with the change of thermal annealing time the slight deviation between the zeta potential of the membranes is likely to be a result of experimental error. However, it is evident similar like SH at pH 7.4 the surfaces of the SH-T24h, SH-T36h and SH-T48h are negatively charged which prevents the adsorption of BSA, Hb and Cat on these membranes (Supporting Information, Table S4).

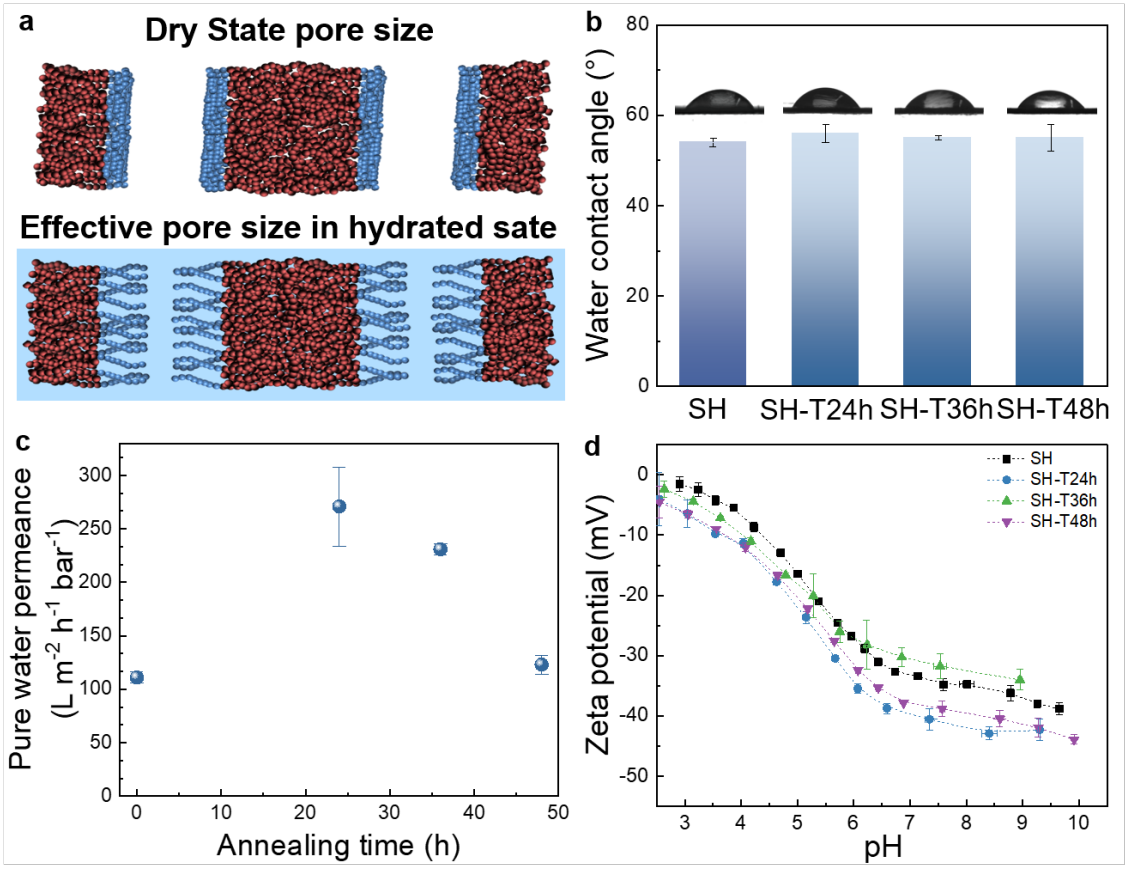

Fig. 8. a) Schematic representation of dry state and hydrated state pores of PS-*b*-PHEMA membranes (SH, SH-T24h, SH-T36h and SH-T48h). Comparison of SH, SH-T24h, SH-T36h and SH-T48h: b) water contact angle at the surface of the membranes, c) water permeance, d) streaming zeta potential at the surface of the membranes.

Fig. 9b shows the retention of Hb through SH, SH-T24h, SH-T36h and SH-T48h are 89%, 27%, 75% and 82%, respectively. This trend of Hb retention supports our assumption of the change of effective pore size of the membrane made from the water permeance i.e. the effective pore size of SH-T24h > SH-T36h > SH-T48h > SH. This change of effective pore size is not big enough to have an impact on the retention of Cat (Fig. 9c) which has a bigger size compared to Hb. However, unlike the retention of Hb, the retention of BSA decreases with the increase of thermal annealing time (Fig. 9a). This leads us to a conjecture that together with the effective pore size the length of the cylindrical pores of SH (179 nm), SH-T24h (132 nm), SH-T36h (103 nm) and SH-T48h (65 nm) had a synergistic influence to determine the trend of the retention of BSA and the permeance of BSA aqueous solution.

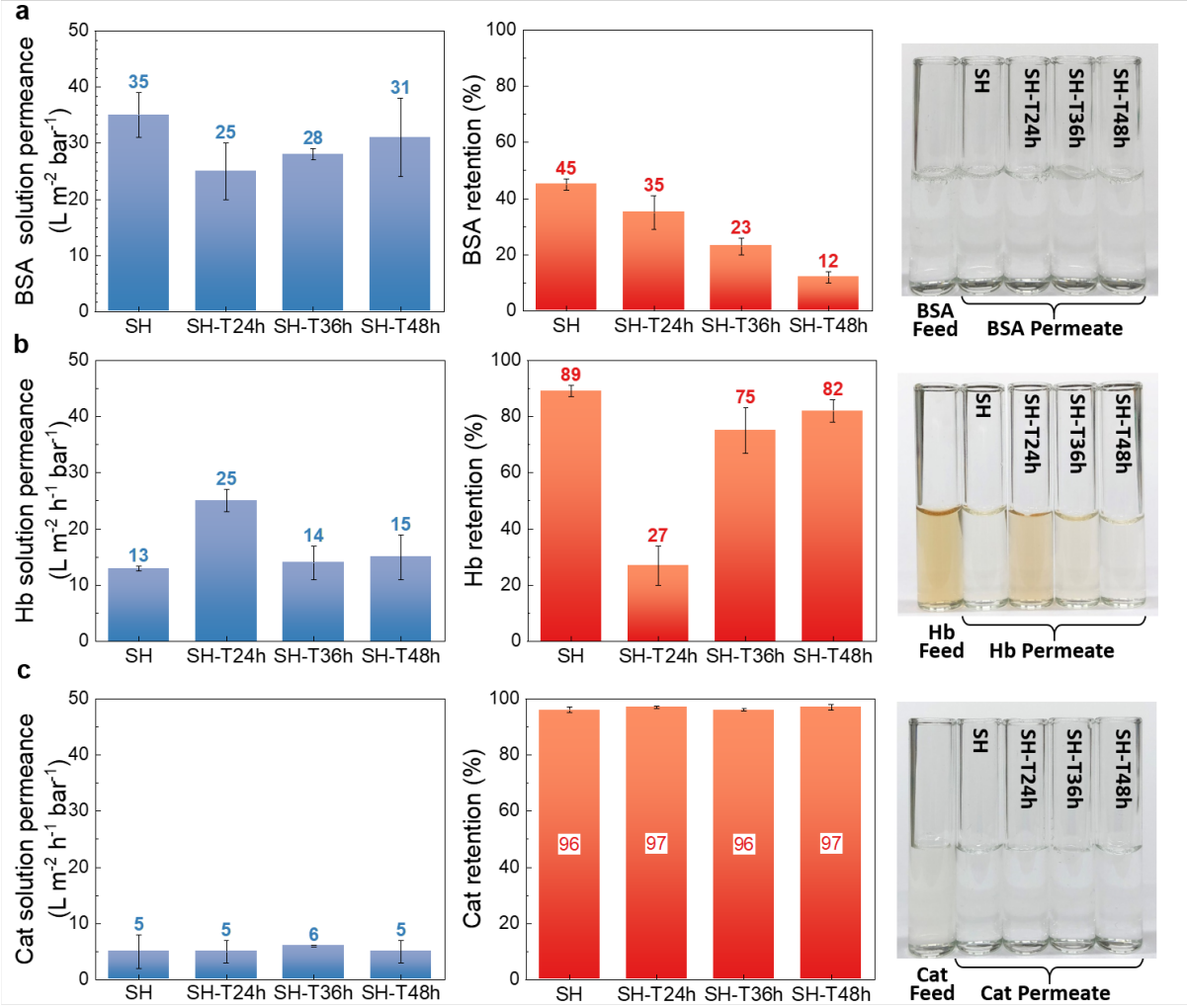

Fig. 9. Protein retention of pristine membrane (SH) and thermally annealed membranes (SH-T) for different times.

3.4. Ideal selectivity of membranes

Fig. 10 shows that the ideal selectivities of the three protein pairs, BSA/Hb ($\psi_{BSA/Hb}$), BSA/Cat ($\psi_{BSA/Cat}$) and Hb/Cat ($\psi_{Hb/Cat}$), can be tuned by both chemical postmodification by urethane chemistry and the physical post treatment by thermal annealing. To benchmark the potential of protein fractionation, the ideal selectivities of 22 commercial and in-house prepared isoporous and non-

isoporous membranes are also plotted in Fig. 10. Among these membranes there are 11 commercial non-isoporous membranes having molecular weight cut-offs between 100 ~ 500 kDa composed of polyacrylonitrile, polyvinylidene fluoride, polyethersulfone, polysulfone and regenerated cellulose, respectively. Additionally there are six non-isoporous polyacrylonitrile membranes prepared in-house using NIPS. There are four commercial isoporous polycarbonate track-etched membranes having nominal pore size of 0.015 ~ 0.1 µm and one commercial anodisc membrane with the nominal pore size of 0.02 µm. The investigation of these 22 membranes composed of different materials and having different nominal pore sizes allowed us to acquire the $\psi_{BSA/Hb}$, $\psi_{BSA/Cat}$ and $\psi_{Hb/Cat}$ for BSA solution permeance between 1 and 52 L m^{-2} h^{-1} bar^{-1}, Hb solution permeance between 1 and 27 L m^{-2} h^{-1} bar^{-1} and Cat solution permeance between 1 and 17 L m^{-2} h^{-1} bar^{-1}. The detailed data of these membranes are provided in Supporting Information (Table S5). Considering the range of BSA, Hb and Cat solutions permeance through the membranes prepared by SNIPS in this work (Fig.6 and Fig.9), these 22 membranes represent a good cross-section of the conventional membranes for comparison. Several of these membranes have $\psi_{BSA/Hb}$, $\psi_{BSA/Cat}$ and $\psi_{Hb/Cat}$ almost equal to 1. It implies these membranes either retain or allow the permeation of both proteins of the respective protein pairs which is not desired for protein fractionation. As the molecular weight of BSA and Hb are almost identical, the $\psi_{BSA/Hb}$ of all the membranes are rather low. The $\psi_{BSA/Hb}$ of SH is 5 which is higher than most of the membranes plotted in Fig. 10a. After chemical postmodification, the $\psi_{BSA/Hb}$ decreased as a result of higher retention for both proteins. Among the thermally annealed membranes only SH-T48h has a $\psi_{BSA/Hb}$ = 5 which is equal to that of SH. The $\psi_{BSA/Cat}$ and the $\psi_{Hb/Cat}$ of the thermally annealed and the chemically postmodified membranes are significantly higher than those of SH. It was not possible to calculate the $\psi_{BSA/Cat}$ and the $\psi_{Hb/Cat}$ of SHE-48h as 100% Cat is retained by this membrane from aqueous solution (Fig. 6c). The $\psi_{BSA/Cat}$ of SH is 15 which is higher than several commercial ultrafiltration membranes plotted in Fig. 10c. The $\psi_{BSA/Cat}$ of all the post treated membranes are higher than SH. SH-T48h has a $\psi_{BSA/Cat}$ = 27 which is the highest among all membranes prepared in this work. The biggest success of this work is the excellent $\psi_{Hb/Cat}$ of the postmodified membranes. The $\psi_{Hb/Cat}$ for SH-T24h and SHE-36h are 28 and 27, respectively, which are nine-fold higher than that of SH. Among the membranes presented here, the $\psi_{BSA/Cat}$ and the $\psi_{Hb/Cat}$ of only one in-house prepared non-isoporous polyacrylonitrile membrane are higher than the postmodfied SNIPS membranes. It is worth mentioning here that the selectivity values of a real mixture of proteins might deviate significantly from the ideal protein selectivity. The real selectivity is largely influenced by the composition of the protein mixtures. Moreover, the proteins have the possibility to attract or repel each other in an aqueous solution containing mixture of proteins. The ideal selectivity values are not influenced by such factors which are inevitable in a protein mixture. Nevertheless, the obtained $\psi_{BSA/Cat}$ and the $\psi_{Hb/Cat}$ values of the prepared membranes prove the potential of using these prepared membranes for protein fractionation, and have an instructive significance on further investigations of the real selectivity values using aqueous solution protein mixtures in the future.

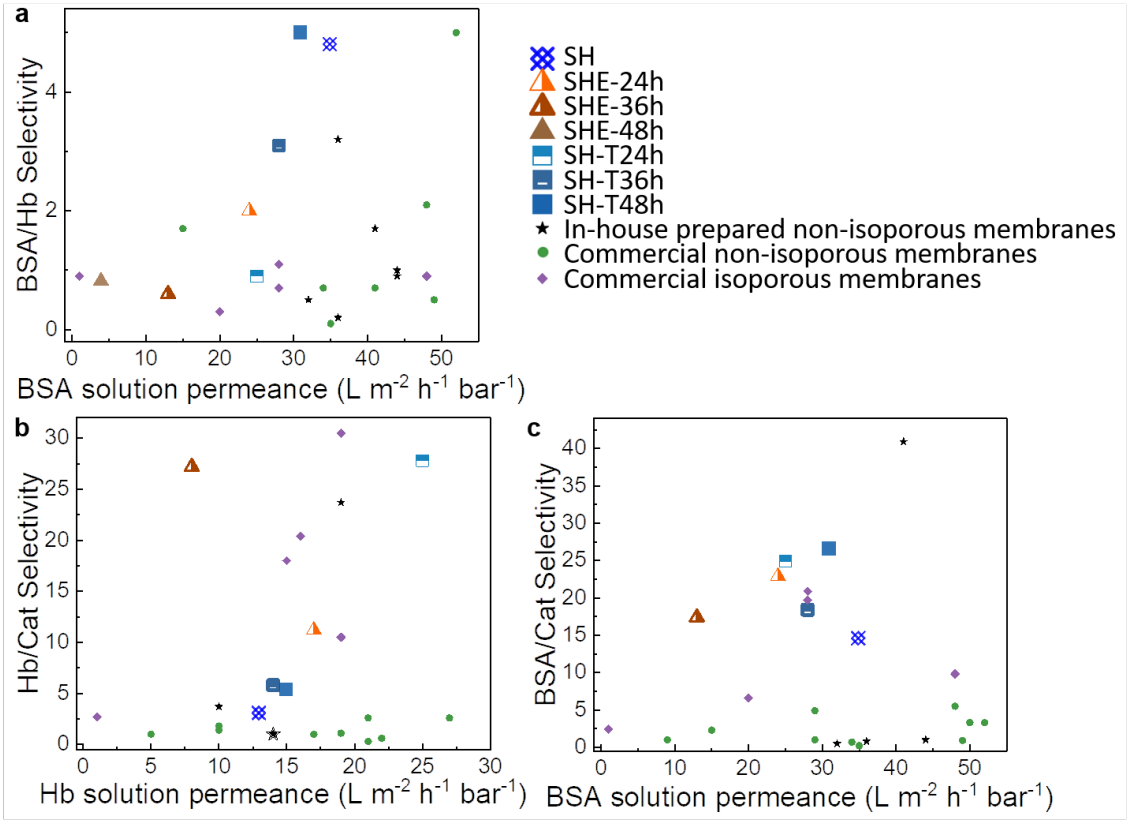

Fig. 10. Comparison of ideal selectivities of the prepared membranes with 22 commercial and in-house prepared isoporous/non-isoporous membranes.

4. Conclusions

We successfully prepared a PS-*b*-PHEMA membrane on the nonwoven support by the SNIPS process and tuned the dry state pore size of the membrane down to 10 nm via two individual methods, the chemical postmodification using an isocyanate and the physical post treatment of thermal annealing. All procedures can be carried out on a large scale. The investigation of water permeance demonstrated the trend of the effective pore size in the hydrated state with the duration of post modification time is different from the changes of the pore sizes in the dry state as obtained from SEM analysis of the surfaces. At pH 7.4 BSA, Hb and Cat do not adsorb at the surface of the membrane. The retention of BSA, Hb and Cat from their aqueous solution are largely (but not only) dictated by the effective pore size of the membranes. From the $\psi_{BSA/Hb}$, the $\psi_{BSA/Cat}$ and the $\psi_{Hb/Cat}$ comparison it is evident that the size selectivity of the PS-*b*-PHEMA membrane changed after both chemical postmodification and thermal annealing. The nine-fold increase of $\psi_{Hb/Cat}$ has been achieved by such methods. This work demonstrates that tuning the size selectivity of the isoporous membrane by adjusting the pore size is a promising way to enhance the ideal selectivity of the protein pairs. As the membrane fabrication technique and the post treatment methods to systematically change the pore size are readily scalable, in our opinion the obtained results demonstrate an important progress for utilization of isoporous block copolymer membranes for protein fractionation.

Acknowledgements

The authors thank Anke-Lisa Höhme, Erik Schneider, Silvio Neumann, Thomas Emmler, Maren Brinkmann and Petra Merten for characterizations of the block copolymer and membranes, Barbara Bajer for the flux, adsorption and retention measurements, and Brigitte Lademann, Jan Wind and Berthold Wendland for technical support.

References

[1] A.L. Zydney, Protein separations using membrane filtration: new opportunities for whey fractionation, Int. Dairy J., 8 (1998) 243-250.

https://doi.org/10.1016/S0958-6946(98)00045-4

[2] A. Saxena, B.P. Tripathi, M. Kumar, V.K. Shahi, Membrane-based techniques for the separation and purification of proteins: An overview, Adv. Colloid Interface Sci., 145 (2009) 1-22.

https://doi.org/10.1016/j.cis.2008.07.004

[3] S. El-Safty, A. Shahat, M.R. Awual, M. Mekawy, Large three-dimensional mesocage pores tailoring silica nanotubes as membrane filters: nanofiltration and permeation flux of proteins, J. Mater. Chem., 21 (2011) 5593-5603.

https://doi.org/10.1039/C0JM03269G

[4] J.-W. Liu, T. Yang, S. Chen, X.-W. Chen, J.-H. Wang, Nickel chelating functionalization of graphene composite for metal affinity membrane isolation of lysozyme, J. Mater. Chem. B, 1 (2013) 810-818.

https://doi.org/10.1039/C2TB00334A

[5] Z. Chen, T. Chen, X. Sun, B.J. Hinds, Dynamic electrochemical membranes for continuous affinity protein separation, Adv. Funct. Mater., 24 (2014) 4317-4323.

https://doi.org/10.1002/adfm.201303707

[6] C. Zhou, T. Segal-Peretz, M.E. Oruc, H.S. Suh, G. Wu, P.F. Nealey, Fabrication of nanoporous alumina ultrafiltration membrane with tunable pore size using block copolymer templates, Adv. Funct. Mater., 27 (2017) 1701756.

https://doi.org/10.1002/adfm.201701756

[7] X. Dou, Q. Wang, Z. Li, J. Ju, S. Wang, L. Hao, K. Sui, Y. Xia, Y. Tan, Seaweed-Derived Electrospun Nanofibrous Membranes for Ultrahigh Protein Adsorption, Adv. Funct. Mater., 29 (2019) 1905610.

https://doi.org/10.1002/adfm.201905610

[8] Z. Cui, Protein separation using ultrafiltration—an example of multi-scale complex systems, China Particuology, 3 (2005) 343-348.

https://doi.org/10.1016/S1672-2515(07)60213-9

[9] S. Saksena, A.L. Zydney, Influence of protein–protein interactions on bulk mass transport during ultrafiltration, J. Membr. Sci., 125 (1997) 93-108.

https://doi.org/10.1016/S0376-7388(96)00132-9

[10] Z. Wang, X. Yao, Y. Wang, Swelling-induced mesoporous block copolymer membranes with intrinsically active surfaces for size-selective separation, J. Mater. Chem., 22 (2012) 20542-20548.

https://doi.org/10.1039/C2JM34292H

[11] D. Musale, S. Kulkarni, Relative rates of protein transmission through poly (acrylonitrile) based ultrafiltration membranes, J. Membr. Sci., 136 (1997) 13-23.

https://doi.org/10.1016/S0376-7388(97)00179-8

[12] B. Cheang, A.L. Zydney, Separation of α-lactalbumin and β-lactoglobulin using membrane ultrafiltration, Biotechnol. Bioeng., 83 (2003) 201-209.

https://doi.org/10.1002/bit.10659

[13] Y. Wan, R. Ghosh, G. Hale, Z. Cui, Fractionation of bovine serum albumin and monoclonal antibody alemtuzumab using carrier phase ultrafiltration, Biotechnol. Bioeng., 90 (2005) 303-315.

https://doi.org/10.1002/bit.20415

[14] M.M. Rohani, A. Mehta, A.L. Zydney, Development of high performance charged ligands to control protein transport through charge-modified ultrafiltration membranes, J. Membr. Sci., 362 (2010) 434-443.

https://doi.org/10.1016/j.memsci.2010.06.069

[15] M.M. Rohani, A.L. Zydney, Protein transport through zwitterionic ultrafiltration membranes, J. Membr. Sci., 397 (2012) 1-8.

https://doi.org/10.1016/j.memsci.2011.12.021

[16] M. Sorci, M. Gu, C.L. Heldt, E. Grafeld, G. Belfort, A multi-dimensional approach for fractionating proteins using charged membranes, Biotechnol. Bioeng., 110 (2013) 1704-1713.

https://doi.org/10.1002/bit.24837

[17] A.S. Bhadouria, M. Sorci, M. Gu, G. Belfort, J. Hahn, Optimization of membrane separation processes for protein fractionation, Ind. Eng. Chem. Res., 53 (2014) 5103-5109.

https://doi.org/10.1021/ie401303d

[18] K.V. Peinemann, V. Abetz, P.F. Simon, Asymmetric superstructure formed in a block copolymer via phase separation, Nat. Mater., 6 (2007) 992-996.

https://doi.org/10.1038/nmat2038

[19] W.A. Phillip, B. O'Neill, M. Rodwogin, M.A. Hillmyer, E. Cussler, Self-assembled block copolymer thin films as water filtration membranes, ACS Appl. Mater. Interfaces, 2 (2010) 847-853.

https://doi.org/10.1021/am900882t

[20] V. Abetz, Isoporous block copolymer membranes, Macromol. Rapid Commun., 36 (2015) 10-22.

https://doi.org/10.1002/marc.201400556

[21] X. Qiu, H. Yu, M. Karunakaran, N. Pradeep, S.P. Nunes, K.-V. Peinemann, Selective Separation of Similarly Sized Proteins with Tunable Nanoporous Block Copolymer Membranes, ACS Nano, 7 (2013) 768–776.

https://doi.org/10.1021/nn305073e

[22] J. Hahn, J.I. Clodt, V. Filiz, V. Abetz, Protein separation performance of self-assembled block copolymer membranes, RSC Adv., 4 (2014) 10252.

https://doi.org/10.1039/C3RA47306F

[23] G.-d. Zhu, Y.-r. Ying, X. Li, Y. Liu, C.-y. Yang, Z. Yi, C.-j. Gao, Isoporous membranes with sub-10 nm pores prepared from supramolecular interaction facilitated block copolymer assembly and application for protein separation, J. Membr. Sci., 566 (2018) 25-34.

https://doi.org/10.1016/j.memsci.2018.08.033

[24] R. Shevate, M. Kumar, H. Cheng, P.Y. Hong, A.R. Behzad, D. Anjum, K.V. Peinemann, Rapid Size-Based Protein Discrimination inside Hybrid Isoporous Membranes, ACS Appl. Mater. Interfaces, 11 (2019) 8507-8516.

https://doi.org/10.1021/acsami.8b20802

[25] J. Wang, M.M. Rahman, C. Abetz, V. Abetz, Bovine serum albumin selective integral asymmetric isoporous membrane, J. Membr. Sci., 604 (2020) 118074.

https://doi.org/10.1016/j.memsci.2020.118074

[26] J. Hahn, J.I. Clodt, C. Abetz, V. Filiz, V. Abetz, Thin isoporous block copolymer membranes: it is all about the process, ACS Appl. Mater. Interfaces, 7 (2015) 21130-21137.

https://doi.org/10.1021/acsami.5b04658

[27] T. Bucher, V. Filiz, C. Abetz, V. Abetz, Formation of thin, isoporous block copolymer membranes by an upscalable profile roller coating process—A promising way to save block copolymer, Membranes, 8 (2018) 57.

https://doi.org/10.3390/membranes8030057

[28] M. Radjabian, J. Koll, K. Buhr, U. Vainio, C. Abetz, U.A. Handge, V. Abetz, Tailoring the morphology of self-assembled block copolymer hollow fiber membranes, Polymer, 55 (2014) 2986-2997.

https://doi.org/10.1016/j.polymer.2014.04.041

[29] N. Noor, J. Koll, M. Radjabian, C. Abetz, V. Abetz, A Facile Method to Prepare Double-Layer Isoporous Hollow Fiber Membrane by In Situ Hydrogen Bond Formation in the Spinning Line, Macromol. Rapid Commun., 37 (2016) 414-419.

https://doi.org/10.1002/marc.201500593

[30] K. Sankhala, J. Koll, M. Radjabian, U.A. Handge, V. Abetz, A Pathway to Fabricate Hollow Fiber Membranes with Isoporous Inner Surface, Adv. Mater. Interfaces, 4 (2017) 1600991.

https://doi.org/10.1002/admi.201600991

[31] M. Radjabian, V. Abetz, Advanced Porous Polymer Membranes from Self-Assembling Block Copolymers, Prog. Polym. Sci., (2020) 101219.

https://doi.org/10.1016/j.progpolymsci.2020.101219

[32] J. Hahn, V. Filiz, S. Rangou, B. Lademann, K. Buhr, J.I. Clodt, A. Jung, C. Abetz, V. Abetz, PtBS-*b*-P4VP and PTMSS-*b*-P4VP Isoporous Integral-Asymmetric Membranes with High Thermal and Chemical Stability, Macromol. Mater. Eng., 298 (2013) 1315-1321.

https://doi.org/10.1002/mame.201300012

[33] A. Jung, S. Rangou, C. Abetz, V. Filiz, V. Abetz, Structure Formation of Integral Asymmetric Composite Membranes of Polystyrene-block-Poly(2-vinylpyridine) on a Nonwoven, Macromol. Mater. Eng., 297 (2012) 790-798.

https://doi.org/10.1002/mame.201100359

[34] J. Hahn, V. Filiz, S. Rangou, J. Clodt, A. Jung, K. Buhr, C. Abetz, V. Abetz, Structure formation of integral-asymmetric membranes of polystyrene-block-poly (ethylene oxide), J. Polym. Sci. Part B: Polym. Phys., 51 (2013) 281-290.

https://doi.org/10.1002/polb.23209

[35] A. Jung, V. Filiz, S. Rangou, K. Buhr, P. Merten, J. Hahn, J. Clodt, C. Abetz, V. Abetz, Formation of integral asymmetric membranes of AB diblock and ABC triblock copolymers by phase inversion, Macromol. Rapid Commun., 34 (2013) 610-615.

https://doi.org/10.1002/marc.201200770

[36] R.M. Dorin, W.A. Phillip, H. Sai, J. Werner, M. Elimelech, U. Wiesner, Designing block copolymer architectures for targeted membrane performance, Polymer, 55 (2014) 347-353.

https://doi.org/10.1016/j.polymer.2013.09.038

[37] R.A. Mulvenna, J.L. Weidman, B. Jing, J.A. Pople, Y. Zhu, B.W. Boudouris, W.A. Phillip, Tunable nanoporous membranes with chemically-tailored pore walls from triblock polymer templates, J. Membr. Sci., 470 (2014) 246-256.

https://doi.org/10.1016/j.memsci.2014.07.021

[38] Z. Zhang, M.M. Rahman, C. Abetz, V. Abetz, High-Performance Asymmetric Isoporous Nanocomposite Membranes with Chemically-Tailored Amphiphilic Nanochannels, J. Mater. Chem. A, 8 (2020) 9554-9566.

https://doi.org/10.1039/D0TA01023E

[39] Z. Zhang, M.M. Rahman, C. Abetz, A.L. Höhme, E. Sperling, V. Abetz, Chemically Tailored Multifunctional Asymmetric Isoporous Triblock Terpolymer Membranes for Selective Transport, Adv. Mater., 32 (2020) 1907014.

https://doi.org/10.1002/adma.201907014

[40] S. Schöttner, H.-J. Schaffrath, M. Gallei, Poly(2-hydroxyethyl methacrylate)-Based Amphiphilic Block Copolymers for High Water Flux Membranes and Ceramic Templates, Macromolecules, 49 (2016) 7286-7295.

https://doi.org/10.1021/acs.macromol.6b01803

[41] S. Saleem, S. Rangou, C. Abetz, B. Lademann, V. Filiz, V. Abetz, Block Copolymer Membranes from Polystyrene-*b*-poly(solketal methacrylate) (PS-*b*-PSMA) and Amphiphilic Polystyrene-*b*-poly(glyceryl methacrylate) (PS-*b*-PGMA), Polymers, 9 (2017) 216.

https://doi.org/10.3390/polym9060216

[42] S. Saleem, S. Rangou, C. Abetz, V. Filiz, V. Abetz, Isoporous Membranes from Novel Polystyrene-b-poly (4-vinylpyridine)-b-poly (solketal methacrylate)(PS-b-P4VP-b-PSMA) Triblock Terpolymers and Their Post-Modification, Polymers, 12 (2020) 41.

https://doi.org/10.3390/polym12010041

[43] S. Rangou, K. Buhr, V. Filiz, J.I. Clodt, B. Lademann, J. Hahn, A. Jung, V. Abetz, Self-organized isoporous membranes with tailored pore sizes, J. Membr. Sci., 451 (2014) 266-275.

https://doi.org/10.1016/j.memsci.2013.10.015

[44] M. Radjabian, V. Abetz, Tailored pore sizes in integral asymmetric membranes formed by blends of block copolymers, Adv. Mater., 27 (2015) 352-355.

https://doi.org/10.1002/adma.201404309

[45] J. Wang, M.M. Rahman, C. Abetz, S. Rangou, Z. Zhang, V. Abetz, Novel Post-Treatment Approaches to Tailor the Pore Size of PS-*b*-PHEMA Isoporous Membranes, Macromol. Rapid Commun., 39 (2018) 1800435.

https://doi.org/10.1002/marc.201800435

[46] H. Yu, X. Qiu, S.P. Nunes, K.V. Peinemann, Self-assembled isoporous block copolymer membranes with tuned pore sizes, Angew. Chem. Int. Ed., 53 (2014) 10072-10076.

https://doi.org/10.1002/anie.201404491

[47] J.I. Clodt, B. Bajer, K. Buhr, J. Hahn, V. Filiz, V. Abetz, Performance study of isoporous membranes with tailored pore sizes, J. Membr. Sci., 495 (2015) 334-340.

https://doi.org/10.1016/j.memsci.2015.07.041

[48] Z. Zhang, M.M. Rahman, C. Abetz, B. Bajer, J. Wang, V. Abetz, Quaternization of a Polystyrene-*block*-poly(4-vinylpyridine) Isoporous Membrane: An Approach to Tune the Pore Size and the Charge Density, Macromol. Rapid Commun., 40 (2018) 1800729.

https://doi.org/10.1002/marc.201800729

[49] X. Yao, Z. Wang, Z. Yang, Y. Wang, Energy-saving, responsive membranes with sharp selectivity assembled from micellar nanofibers of amphiphilic block copolymers, J. Mater. Chem. A, 1 (2013) 7100-7110.

https://doi.org/10.1039/C3TA10690J

[50] B.P. Tripathi, N.C. Dubey, S. Choudhury, F. Simon, M. Stamm, Antifouling and antibiofouling pH responsive block copolymer based membranes by selective surface modification, J. Mater. Chem. B, 1 (2013) 3397-3409.

https://doi.org/10.1039/C3TB20386G

[51] R. Shevate, M. Kumar, M. Karunakaran, C. Canlas, K.-V. Peinemann, Surprising transformation of a block copolymer into a high performance polystyrene ultrafiltration membrane with a hierarchically organized pore structure, J. Mater. Chem. A, 6 (2018) 4337-4345.

https://doi.org/10.1039/C7TA09777H

[52] A. Hirao, H. Kato, K. Yamaguchi, S. Nakahama, Polymerization of monomers containing functional groups protected by trialkylsilyl groups. 5. Synthesis of poly (2-hydroxyethyl methacrylate) with a narrow molecular weight distribution by means of anionic living polymerization, Macromolecules, 19 (1986) 1294-1299.

https://doi.org/10.1021/ma00159a002

[53] Z.F.C. R. Ghosh, Fractionation of BSA and lysozyme using ultrafiltration: effect of pH and membrane pretreatment, J. Membr. Sci., 139 (1998) 17-28.

https://doi.org/10.1016/S0376-7388(97)00236-6

[54] S. Schöttner, M. Brodrecht, E. Uhlein, C. Dietz, H. Breitzke, A.A. Tietze, G. Buntkowsky, M. Gallei, Amine-Containing Block Copolymers for the Bottom-Up Preparation of Functional Porous Membranes, Macromolecules, 52 (2019) 2631-2641.

https://doi.org/10.1021/acs.macromol.8b02758

[55] C.M. Hansen, Hansen solubility parameters: a user's handbook, CRC press, 2007.

[56] D.W. Van Krevelen, K. Te Nijenhuis, Properties of polymers: their correlation with chemical structure; their numerical estimation and prediction from additive group contributions, Elsevier, 2009.

[57] C. Hou, S. Lin, F. Liu, J. Hu, G. Zhang, G. Liu, Y. Tu, H. Zou, H. Luo, Synthesis of poly (2-hydroxyethyl methacrylate) end-capped with asymmetric functional groups via atom transfer radical polymerization, New J. Chem., 38 (2014) 2538-2547.

https://doi.org/10.1039/C3NJ01398G

[58] J.I. Clodt, V. Filiz, S. Rangou, K. Buhr, C. Abetz, D. Höche, J. Hahn, A. Jung, V. Abetz, Double Stimuli-Responsive Isoporous Membranes via Post-Modification of pH-Sensitive Self-Assembled Diblock Copolymer Membranes, Adv. Funct. Mater., 23 (2013) 731-738.

https://doi.org/10.1002/adfm.201202015

Supporting Information

Tuning the size selectivity of isoporous membranes for protein fractionation via two scalable post treatment approaches

Jiali Wang[1], Md. Mushfequr Rahman[1], Clarissa Abetz[1], Volker Abetz[1,2]*

[1]Helmholtz-Zentrum Geesthacht, Institute of Polymer Research, Max-Planck-Str. 1, 21502 Geesthacht, Germany

[2]Universität Hamburg, Institute of Physical Chemistry, Martin-Luther-King-Platz 6, 20146 Hamburg, Germany

*Corresponding author. Email address: volker.abetz@hzg.de

Content

Supporting Notes:

1. Synthesis and characterization of polystyrene-*block*-poly(2-hydroxyethyl methacrylate) (PS-*b*-PHEMA) block copolymer

PS-*b*-PHEMA diblock copolymer was successfully synthesized by sequential anionic polymerization of styrene and trimethylsilyl protected hydroxyethyl methacrylate (HEMA) followed by a subsequent hydrolysis of the trimethylsilyloxy group (Fig. S1a) following a protocol reported before.[1, 2] Due to the different solubility of PS and PHEMA segments, the hydroxyl groups of the PHEMA segments were protected by benzoic anhydride for characterizing the chemical composition, molecular weight and Đ of diblock copolymer. (Fig. S1b) The characteristic peaks of PS-*b*-PHEMA and PS-*b*-P(HEMA-Bz) diblock copolymers were shown in ^{1}H-NMR spectra (Fig. S2).^{1}H-NMR spectra shows 100% conversion of benzoylation. According to the results calculated from ^{1}H-NMR and SEC (Fig. S3), the composition, molecular weight and Đ of PHEMA is well controlled, as listed in Table S1. Therefore, PS_{87}-*b*-$PHEMA_{13}^{180k}$ diblock copolymer where the subscripts denote the weight fractions in % and the superscripts the corresponding molecular weight of the block copolymer in kg mol^{-1} was further used for membrane fabrication by SNIPS method.

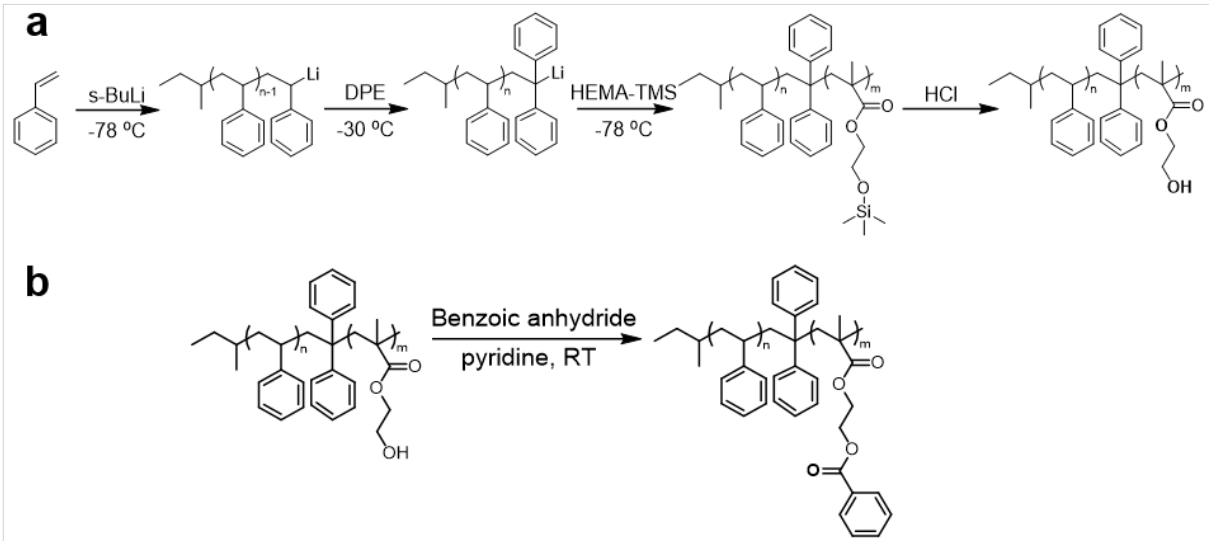

Fig. S1. a) Synthesis scheme of polystyrene-*block*-poly(2-hydroxyethyl methacrylate) (PS-*b*-PHEMA) block copolymer in tetrahydrofuran (THF) by sequential anionic polymerization of styrene and 2-(trimethylsilyloxy)ethyl methacrylate and subsequent hydrolysis. b) Benzoylation of PS-*b*-PHEMA.

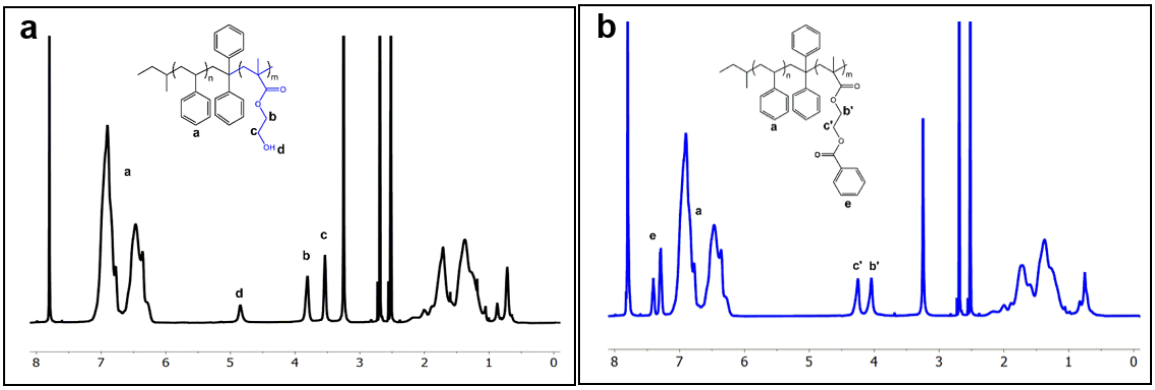

Fig. S2. ^{1}H-NMR spectra of a) PS-*b*-PHEMA and b) PS-*b*-P(HEMA-Bz) in DMF-d7.

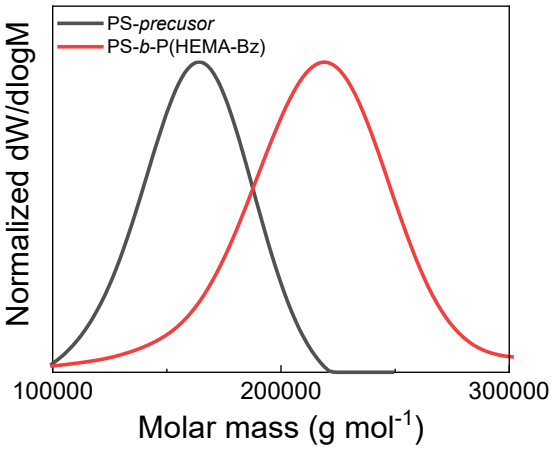

Fig. S3. Molecular weight distribution of PS-*b*-PHEMA and PS-*b*-P(HEMA-Bz) characterized by SEC using PS standards in THF.

Table S1. Characterization of PS-*b*-PHEMA and PS-*b*-P(HEMA-Bz) diblock copolymers by SEC with PS standard in THF.

Polymer [a]	M_n [g mol^{-1}]	M_w [g mol^{-1}]	$Đ$
PS-*precursor*	156 500	159 300	1.018
PS_{93}-*b*-P(HEMA-Bz)$_7$	196 000	206 000	1.051
PS_{88}-*b*-$PHEMA_{12}$ [b]	178 444	---	---
PS_{87}-*b*-$PHEMA_{13}$ [c]	179 885	---	---

[a] Subscripts indicate weight fraction (%) of the blocks.
[b] Molecular weight is calculated by equivalent molar ratio of PS-*b*-P(HEMA-Bz) from SEC.
[c] Molecular weight is calculated from ^{1}H-NMR in DMF-d7 based on PS-precursor molecular weight from SEC;

The bulk morphology of PS_{87}-*b*-$PHEMA_{13}^{180k}$ was investigated by Transmission electron microscopy (TEM). TEM was performed on a Tecnai G^2 F20 (FEI, Eindhoven, The Netherlands) operated at 120 kV in bright-field mode. The samples were prepared from a 5 wt % PS-*b*-PHEMA block copolymer solution in THF, followed by slowly evaporating the solvent at room temperature in the desiccator and subsequently annealing at 130 °C in a vacuum oven. The temperature was slowly increased from room temperature to the targeted temperature over three days and then the final temperature was maintained for 12 hours to ensure the sufficient annealing. The samples were embedded in an epoxy resin. A Leica Ultramicrotome EM UCT (Leica Microsystems, Wetzlar, Germany) equipped with a diamond knife (Diatome AG, Biel, Switzerland) was used for ultrathin sectioning of the samples with a thickness of roughly 50 nm. The PHEMA segments were selectively stained by osmium tetroxide for high-contrast staining. The TEM micrographs of bulk films were analyzed by DigitalMicrograph (Gatan, Pleasanton, USA). In Fig. S4, the TEM micrograph depicts the spherical morphology after staining. The dark domains were PHEMA segments which were selectively stained by osmium tetroxide and the bright domains were PS segments. The diameter of the darker domains was 10 ± 2 nm and the distance between two neighboring dark domains is approximately 30 ± 1 nm.

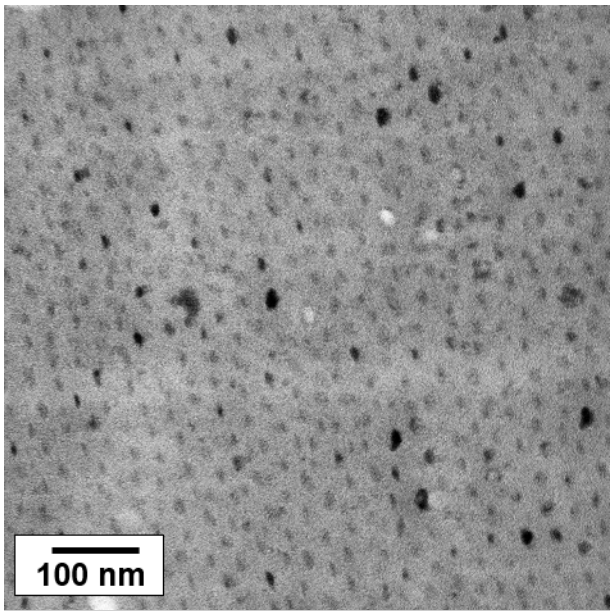

Fig. S4. TEM micrograph of PS_{87}-*b*-$PHEMA_{13}^{180k}$ bulk morphology.

2. Fabrication of PS-*b*-PHEMA diblock copolymer membranes by SNIPS

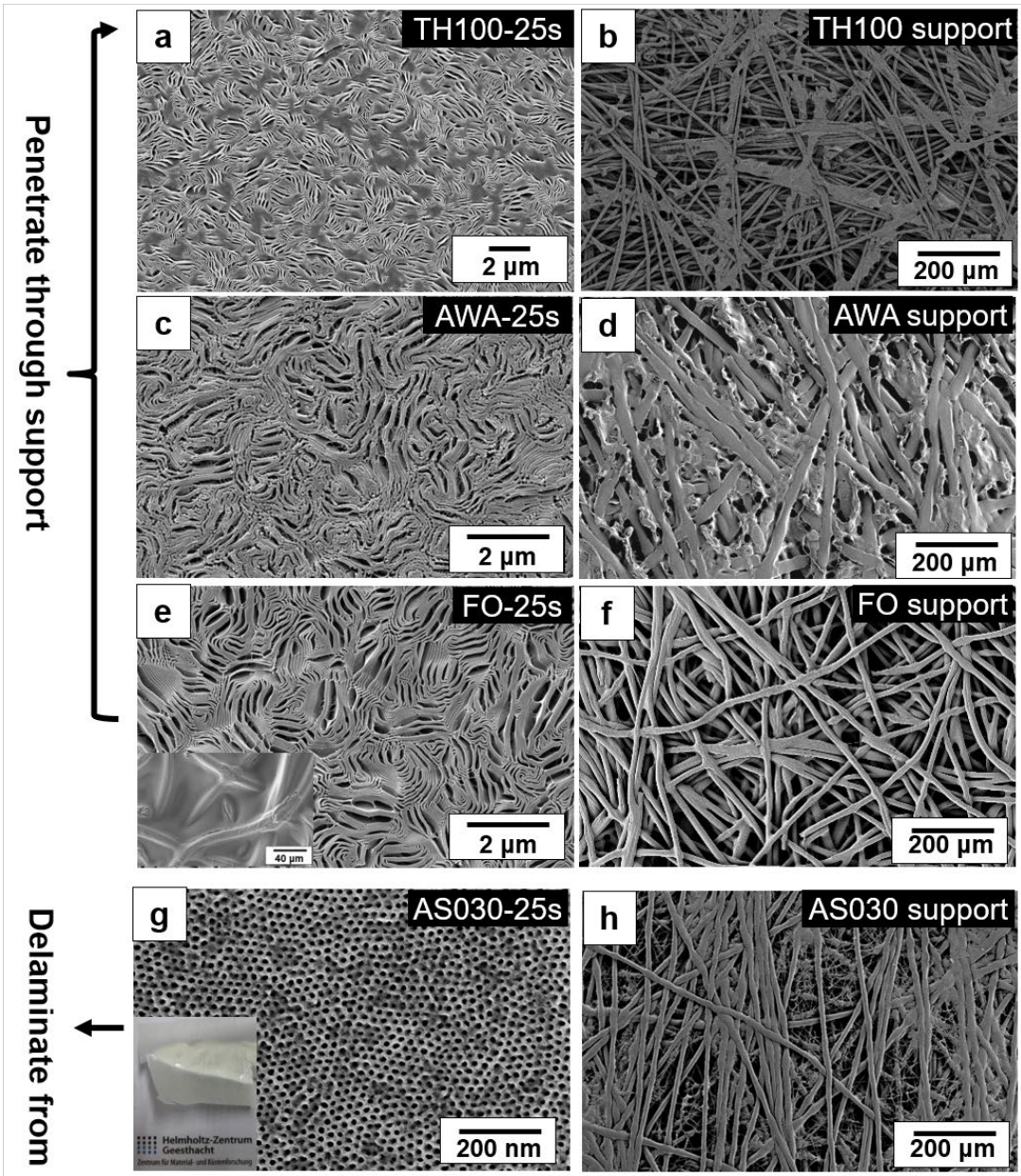

Name of support	Material	Manufacturer
TH100	Polyester (PET)	Hirose
AWA	Polyester (PET)	AWA
FO	Polyethylene/ Polypropylene (PE/PP)	Hirose
AS030	Polyester (PET)	AsahiKasei

Fig. S5. SEM images of PS_{91}-*b*-$PHEMA_9^{97k}$ membrane cast on TH100, AWA, FO and AS030 nonwoven support from 18 wt % solution in DMF/THF/DOX (1:2:1) at the evaporation time of 25 s.

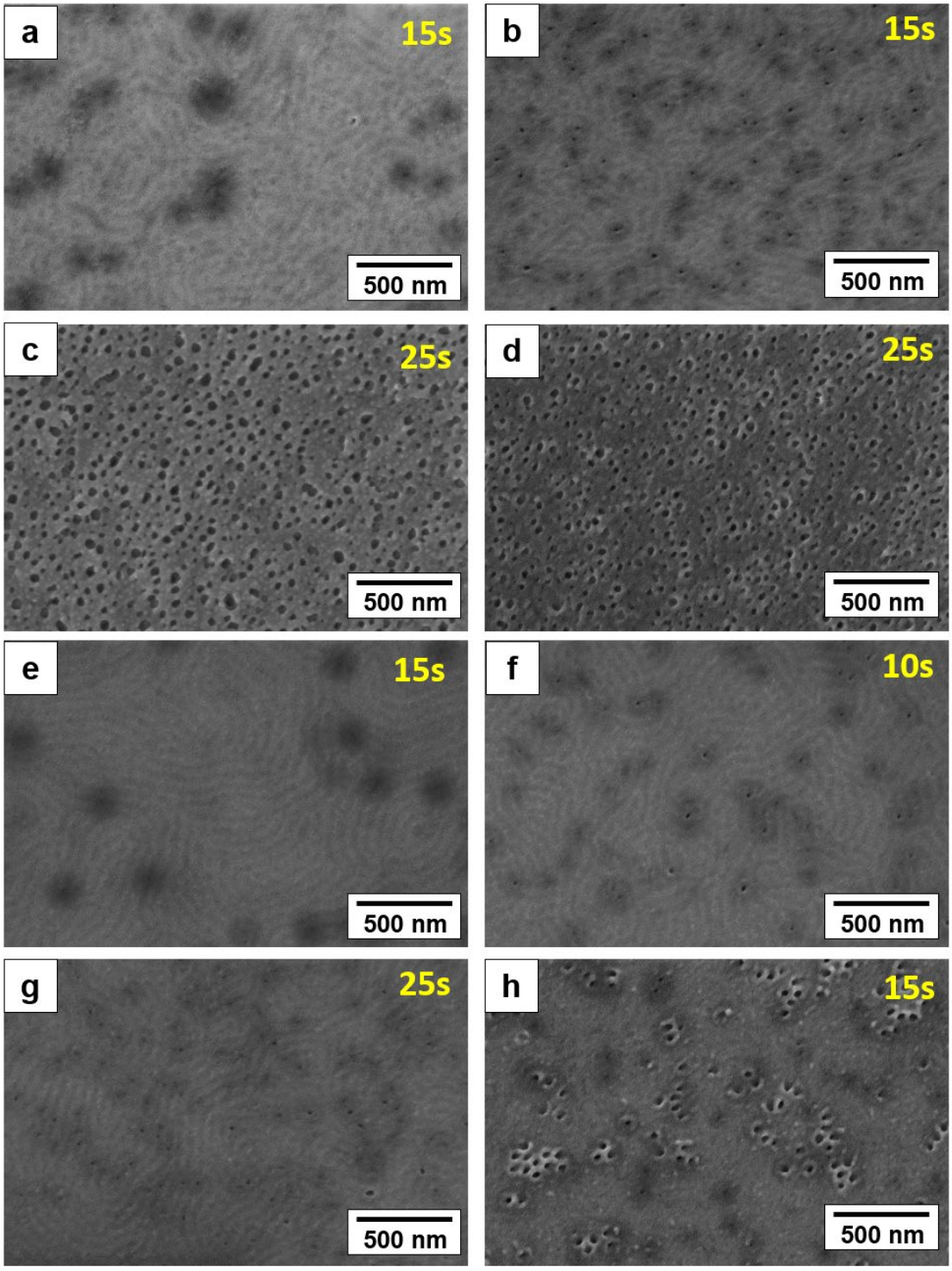

Fig. S6. SEM images of membrane surface prepared from a) 18 wt % PS_{87}-*b*-$PHEMA_{13}^{180k}$ polymer solution in DMF/THF/DOX (1:2:1) at the evaporation time of 15 s; b) 18 wt % PS_{87}-*b*-$PHEMA_{13}^{180k}$ polymer solution in DMF/THF/DOX (1:1:2) at the evaporation time of 15 s; c) 18 wt % PS_{87}-*b*-$PHEMA_{13}^{180k}$ polymer solution in DMF/THF/DOX (1:1:1) at the evaporation time of 25 s; d) 17 wt % PS_{87}-*b*-$PHEMA_{13}^{180k}$ polymer solution in DMF/THF/DOX (1:1:1) at the evaporation time of 25 s; e) 19 wt % PS_{87}-*b*-$PHEMA_{13}^{180k}$ polymer solution in DMF/THF/DOX (1:1:1) at the evaporation time of 15 s; f) 20 wt % PS_{87}-*b*-$PHEMA_{13}^{180k}$ polymer solution in DMF/THF/DOX (1:1:1) at the evaporation time of 10 s; g) 18 wt % PS_{87}-*b*-$PHEMA_{13}^{180k}$ polymer solution in DMF/THF/DOX (1:1:1) at the evaporation time of 25 s with the addition of 0.1 wt % $MgAc_2$; h) 18 wt % PS_{87}-*b*-$PHEMA_{13}^{180k}$ polymer solution in DMF/THF/DOX (1:1:1) at the evaporation time of 15 s with the addition of 0.1 wt % $CuAc_2$.

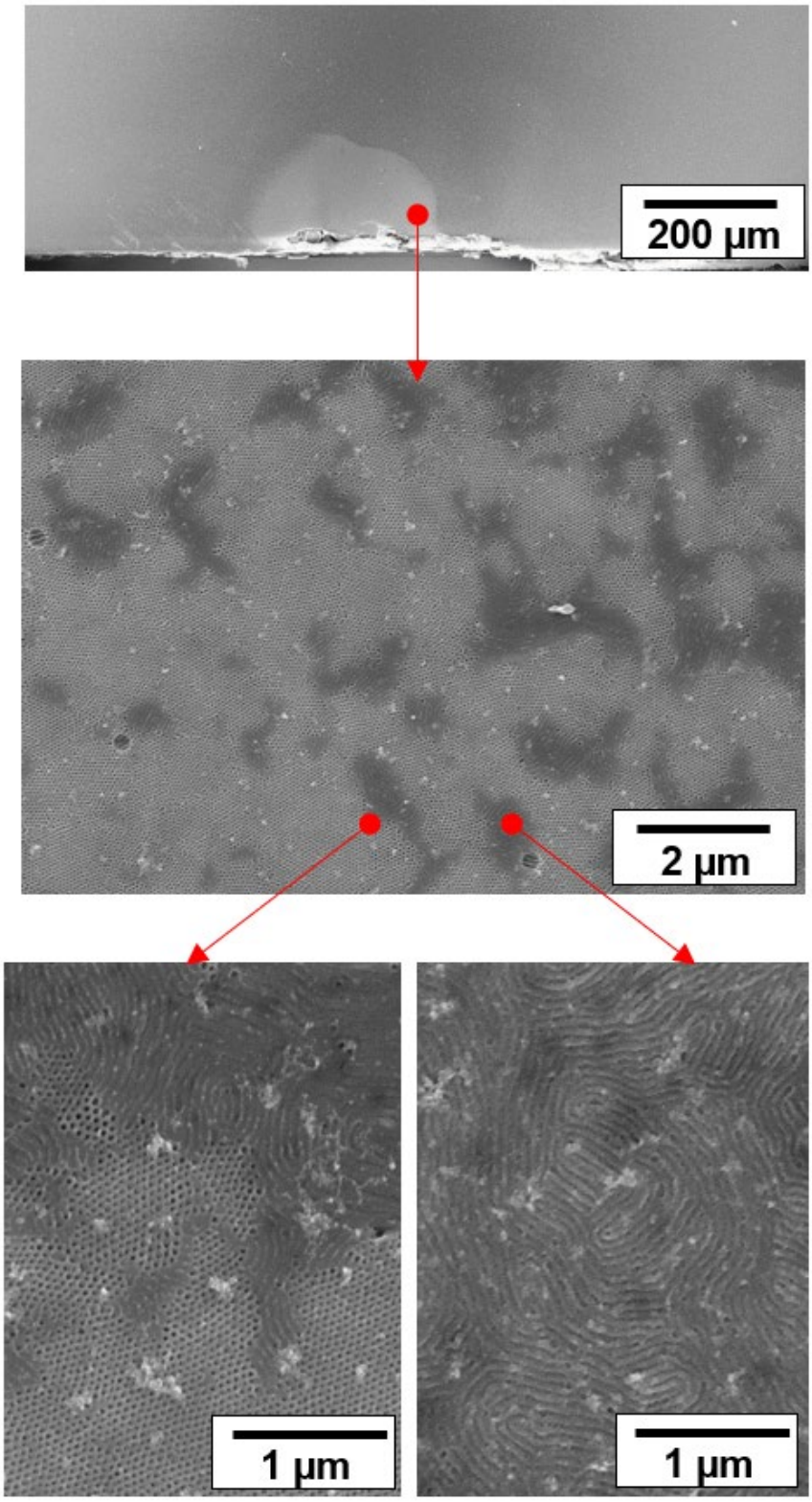

Fig. S7. SEM images of inhomogeneous surface morphology of a membrane prepared from a 21 wt% PS_{87}-*b*-$PHEMA_{13}^{180k}$ solution in DMF/THF/DOX (1:1:1) containing 0.4 wt % $CuAc_2$ at the evaporation time of 20 s.

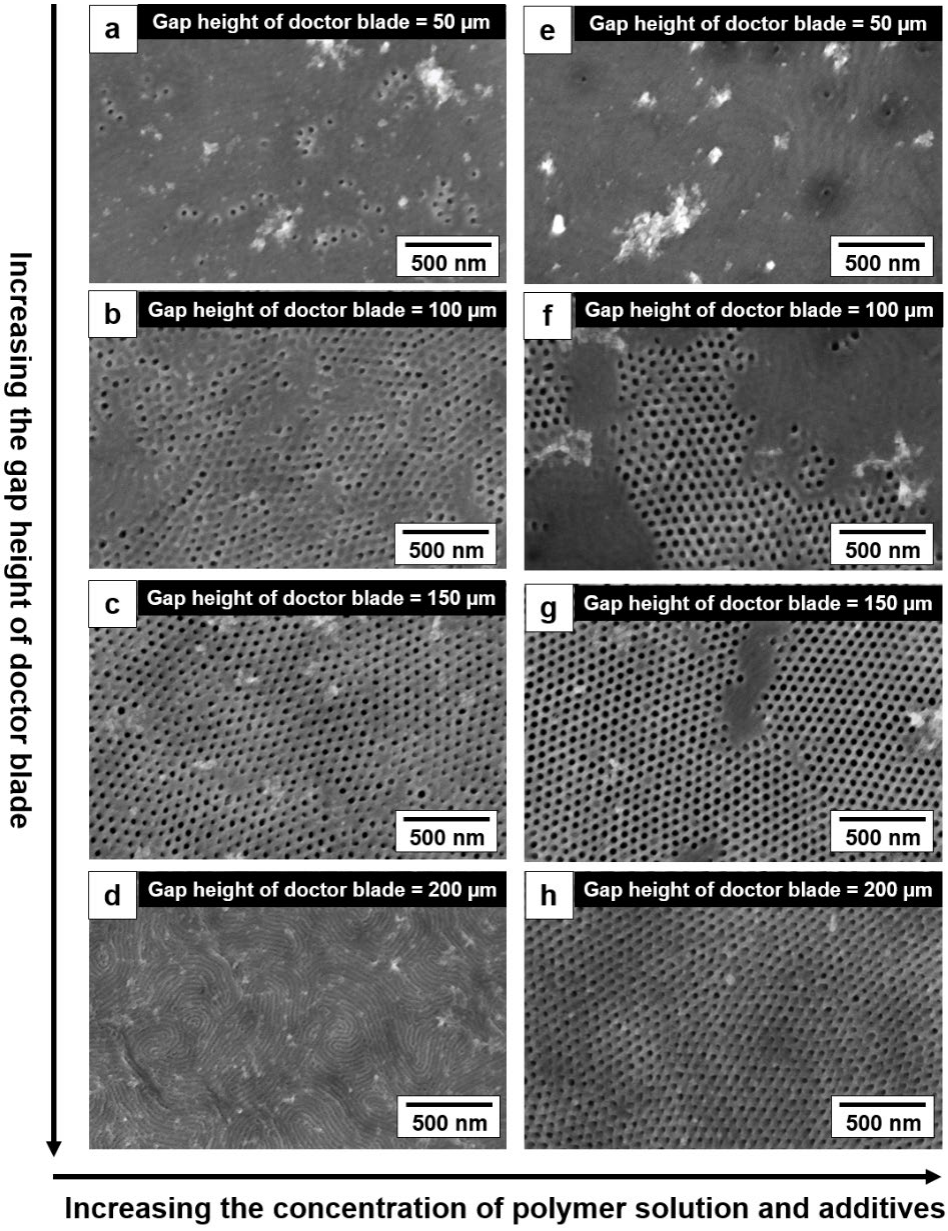

Fig. S8. SEM images of membrane surface prepared from a-d) 20 wt % PS_{87}-*b*-$PHEMA_{13}^{180k}$ polymer solution in DMF/THF/DOX (1:1:1) at the evaporation time of 15 s with the addition of 0.3 wt % $CuAc_2$ cast on the nonwoven support using the gap height of 50 ~ 200 µm; e-h) 21 wt % PS_{87}-*b*-$PHEMA_{13}^{180k}$ polymer solution in DMF/THF/DOX (1:1:1) at the evaporation time of 15 s with the addition of 0.4 wt % $CuAc_2$ cast on the nonwoven support using the gap height of 50 ~ 200 µm.

3. Post treatment of PS-*b*-PHEMA diblock copolymer membranes by urethane chemistry and thermal annealing

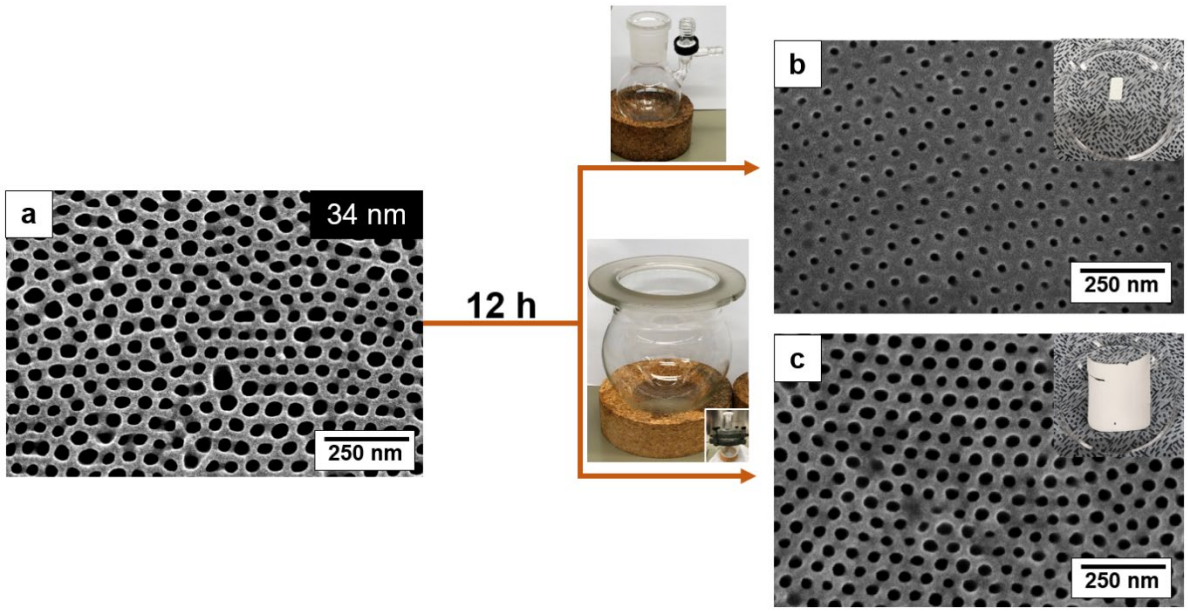

Fig. S9. SEM images of a) PS-*b*-PHEMA pristine membrane; PS-*b*-P(HEMA-*r*-ECEMA) membranes postmodified by ethyl isocyanate at 65 °C for 12 h using b) 25 mL Schlenk flask and c) 500 mL reactor.

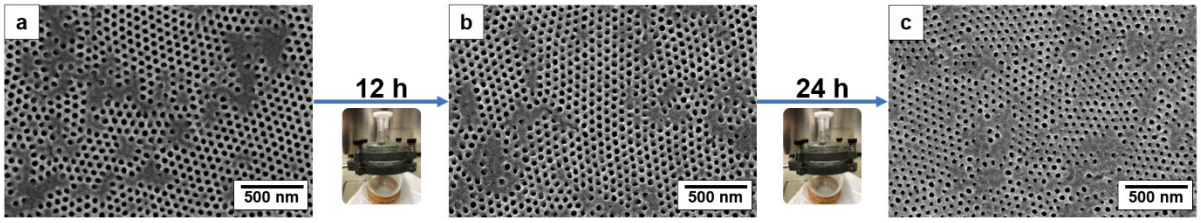

Fig. S10. SEM images of a) PS-*b*-PHEMA pristine membrane; membranes annealed in perfluoro(methyl cyclohexane) using 500 mL reactor at 75 °C for b) 12 h and c) 24 h.

The volume of polymer in such a unit (V_u) can be calculated by subtracting the volume of 3 cylindrical pores ($3V_{pore}$) from the volume of a hexagon ($V_{hexagon}$) (**Fig. S11a**).

$$V_u = V_{hexagon} - 3V_{pore} \quad (1)$$

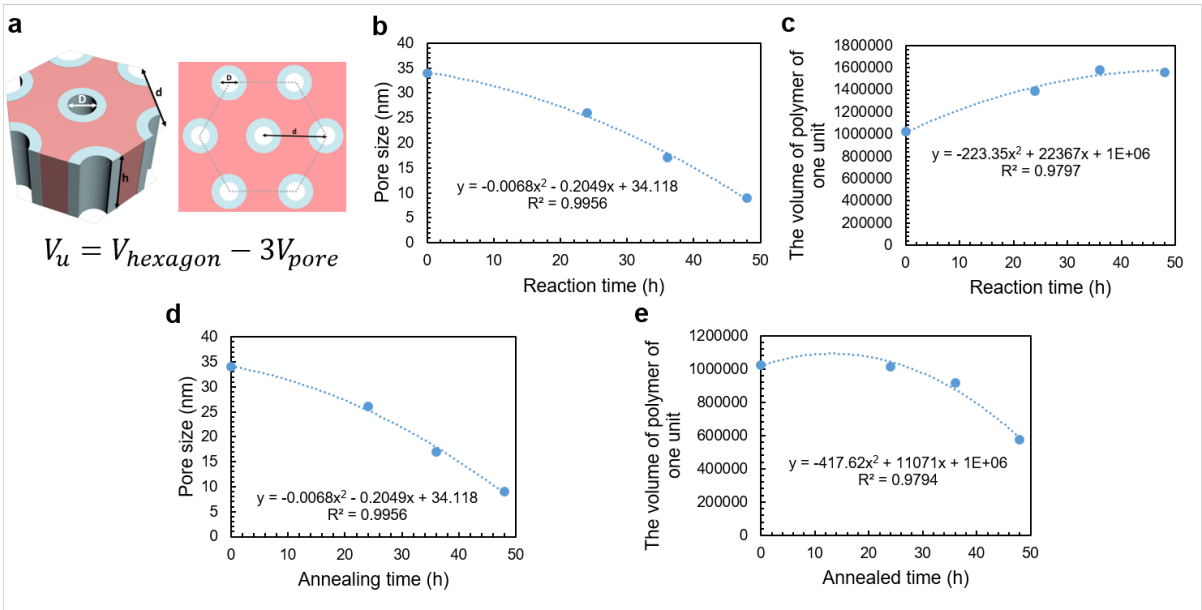

Fig. S11. a) Schematic representation of a hexagonal unit of the isoporous layer of the membrane. Where *h* is the height of the cylinders, *D* is the pore diameter and *d* is the center-to-center distance between two neighboring pores; b) the mean pore size diameter of PS-*b*-PHEMA and PS-*b*-P(HEMA-*r*-ECEMA) membranes as a function of the reaction time; c) The volume of the polymer in one hexagonal unit as a function of reaction time; d) the mean pore size diameter of membranes as a function of annealing time within 48 h at 75 °C; e) the volume of the polymer in one hexagonal unit as a function of annealing time.

4.Membrane performance

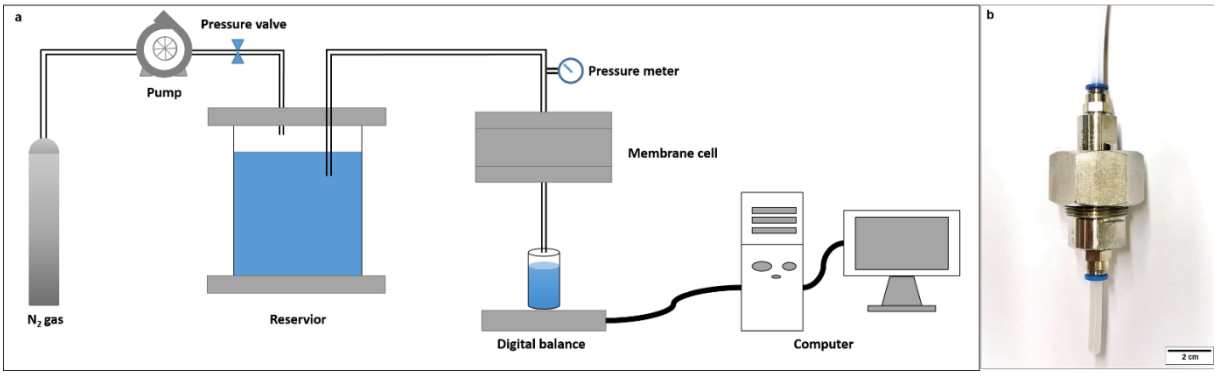

Fig. S12. a) Schematic representation of the experimental setup involving dead-end filtration system; b) membrane cell

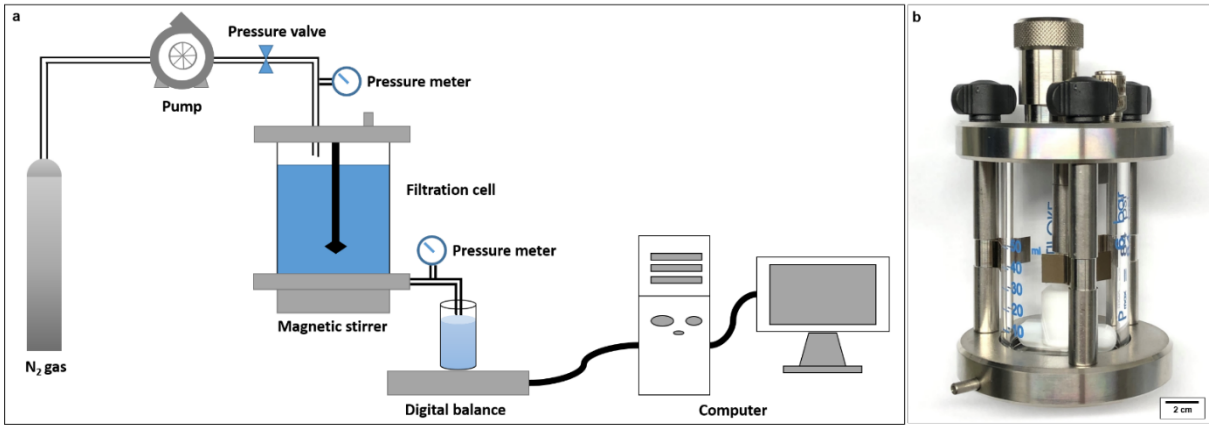

Fig. S13. a) Schematic representation of the experimental setup involving dead-end filtration system; b) membrane filtration cell.

Table S2. Protein physical characteristics.

Characteristics	Proteins		
	Bovine serum albumin	**Hemoglobin**	**Catalase**
Source	Bovine serum	Bovine blood	Bovine liver
Molecular weight [a] [kDa]	66	65	250
Molecular size [nm]	14 × 4 × 4[3]	7 × 5.5 × 5.5[3]	9.7 × 9.2 × 6.7[4]
Isoelectric point	4.7[3]	7.1[3]	5.4[a,[5]]
Hydrophilic amino acid content (g / 100 g protein)[3]	56.16	43.13	---
Protein charge at pH 7.4[3]	-20.5	-4.0	---

[a] Suppliers data (Sigma-Aldrich)

Table S3. Adsorption of proteins on different membranes.

Membranes	Adsorption of proteins [μg cm^{-2}]		
	Bovine serum albumin	**Hemoglobin**	**Catalase**
SH	0	0	0
SHE-24h	0	0	0
SHE-36h	0	0	0
SHE-48h	0	0	0

Table S4. Adsorption of proteins on different membranes.

Membranes	Adsorption of proteins [μg cm^{-2}]		
	Bovine serum albumin	**Hemoglobin**	**Catalase**
SH	0	0	0
SH-T24h	0	0	0
SH-T36h	0	0	0
SH-T48h	0	0	0

Table S5. Protein permeance and ideal selectivity of commercial and in-house prepared isoporous/non-isoporous membranes in 1 g/L feed solution at pH 7.4.[6]

Membranes	Manufacturer	BSA solution permeance [L h^{-1} m^{-2} bar^{-1}]	Hb solution permeance [L h^{-1} m^{-2} bar^{-1}]	Cat solution permeance [L h^{-1} m^{-2} bar^{-1}]	$\psi_{BSA/Hb}$	$\psi_{Hb/Cat}$	$\psi_{BSA/Cat}$
Anodisc - aluminum oxide	Whatman	48 ± 1	19 ± 2	9 ± 4	0.9	10.5	9.8
PC_0.015 - polycarbonate	Whatman	1 ± 0	1 ± 0	1 ± 0	0.9	2.7	2.4
PC_0.05 - polycarbonate	Whatman	28 ± 4	19 ± 4	8 ± 0	0.7	30.5	20.9
PC_0.08 - polycarbonate	Whatman	28 ± 2	15 ± 0	9 ± 2	1.1	18.0	19.7
PC_0.1 - polycarbonate	Whatman	20 ± 2	16 ± 1	7 ± 1	0.3	20.4	6.6
PAN-19/002 - polyacrylonitrile	In-house prepared[a]	32 ± 2	14 ± 7	8 ± 0	0.5	1.0	0.5
PAN-02/141 - polyacrylonitrile	In-house prepared[a]	36 ± 3	10 ± 1	10 ± 1	0.2	3.7	0.8
H-PAN-01/87 - polyacrylonitrile	In-house prepared[a]	44 ± 3	15 ± 4	11 ± 3	0.9	--	--
PAN-HV2-5 - polyacrylonitrile	In-house prepared[a]	44 ± 4	14 ± 3	12 ± 2	1.1	0.6	0.7
PAN-8 - polyacrylonitrile	In-house prepared[a]	36 ± 2	14 ± 2	6 ± 2	3.2	--	--
PAN-6 - polyacrylonitrile	In-house prepared[a]	41 ±9	19 ± 0	9 ± 2	1.7	23.7	40.9
PAN_PY - polyacrylonitrile	Sterlitech	15 ± 5	10 ± 5	12 ± 2	1.7	1.4	2.3
PAN_PX - polyacrylonitrile	Sterlitech	34 ± 4	19 ± 3	17 ± 10	0.7	1.1	0.7
PSUH - polysulfone	Sterlitech	49 ± 12	10 ± 1	7 ± 2	0.5	1.8	0.9
PES_LY - polyethersulfone	Sterlitech	41 ± 5	11 ± 2	10 ± 0	0.7	--	--
PES_UE - polyethersulfone	Sterlitech	9 ± 1	5 ± 1	7 ± 1	--	0.6	2.4
PES_LX - polyethersulfone	Sterlitech	29 ± 4	11 ± 0	8 ± 1	--	--	4.9
PVDF_V5 - polyvinylidene fluoride	Sterlitech	52 ± 15	22 ± 4	13 ± 1	5.0	0.6	3.3
PVDF_BX - polyvinylidene fluoride	Sterlitech	48 ± 4	27 ± 5	7 ± 2	2.1	2.6	5.5
PVDF_A6 - polyvinylidene fluoride	Sterlitech	50 ± 12	21 ± 1	8 ± 0	--	0.3	3.3

PVDF_V6 - polyvinylidene fluoride	Sterlitech	29 ± 4	17 ± 4	10 ± 1	--	0.2	0.5
RC - regenerated cellulose	Sterlitech	35 ± 4	21 ± 4	13 ± 6	0.1	2.6	0.2

[a] The PAN membranes were prepared by Helmholtz-Zentrum Geesthacht.

References

[1] A. Hirao, H. Kato, K. Yamaguchi, S. Nakahama, Polymerization of monomers containing functional groups protected by trialkylsilyl groups. 5. Synthesis of poly (2-hydroxyethyl methacrylate) with a narrow molecular weight distribution by means of anionic living polymerization, Macromolecules, 19 (1986) 1294-1299.
[2] J. Wang, M.M. Rahman, C. Abetz, S. Rangou, Z. Zhang, V. Abetz, Novel Post-Treatment Approaches to Tailor the Pore Size of PS-b-PHEMA Isoporous Membranes, Macromol. Rapid Commun., 39 (2018) 1800435.
[3] S.P. Palecek, A.L. Zydney, Hydraulic permeability of protein deposits formed during microfiltration: effect of solution pH and ionic strength, J. Membr. Sci., 95 (1994) 71-81.
[4] H.P. Erickson, Size and shape of protein molecules at the nanometer level determined by sedimentation, gel filtration, and electron microscopy, Biol. Proced. Online, 11 (2009) 32-51.
[5] T. Samejima, M. Kamata, K. Shibata, Dissociation of bovine liver catalase at low pH, The Journal of Biochemistry, 51 (1962) 181-187.
[6] J. Wang, M.M. Rahman, C. Abetz, V. Abetz, Bovine serum albumin selective integral asymmetric isoporous membrane, J. Membr. Sci., 604 (2020) 118074.